frontiers | Frontiers in Marine Science

TYPE Original Research
PUBLISHED 15 October 2024
DOI 10.3389/fmars.2024.1421769

Check for updates

OPEN ACCESS

EDITED BY
Jesus L. Romalde,
University of Santiago de Compostela, Spain

REVIEWED BY
Kathleen Cusick,
Baltimore County, United States
Laura Martinez Alvarez,
University of Copenhagen, Denmark

*CORRESPONDENCE
Rafael R. de la Haba
rrh@us.es

RECEIVED 23 April 2024
ACCEPTED 11 September 2024
PUBLISHED 15 October 2024

CITATION
Straková D, Sánchez-Porro C, de la Haba RR and Ventosa A (2024) Unveiling the genomic landscape and adaptive mechanisms of the haloarchaeal genus *Halogeometricum*: spotlight on thiamine biosynthesis. *Front. Mar. Sci.* 11:1421769. doi: 10.3389/fmars.2024.1421769

COPYRIGHT
© 2024 Straková, Sánchez-Porro, de la Haba and Ventosa. This is an open-access article distributed under the terms of the Creative Commons Attribution License (CC BY). The use, distribution or reproduction in other forums is permitted, provided the original author(s) and the copyright owner(s) are credited and that the original publication in this journal is cited, in accordance with accepted academic practice. No use, distribution or reproduction is permitted which does not comply with these terms.

Unveiling the genomic landscape and adaptive mechanisms of the haloarchaeal genus *Halogeometricum*: spotlight on thiamine biosynthesis

Dáša Straková, Cristina Sánchez-Porro, Rafael R. de la Haba* and Antonio Ventosa

Department of Microbiology and Parasitology, Faculty of Pharmacy, University of Sevilla, Sevilla, Spain

Recent advances in molecular and metagenomic analyses have enhanced the ability to precisely determine the microbiota of hypersaline environments of marine origin, such as solar salterns, saline lakes, and hypersaline soils, uncovering numerous yet-to-be-isolated prokaryotic groups. Our research focused on the hypersaline ecosystems within the Odiel Saltmarshes, a natural tidal wetland situated at the confluence of the Odiel and Tinto rivers in Huelva province, Southwestern Spain. Employing culture-dependent techniques, we aimed to isolate and characterize novel halophilic prokaryotes from this area. Two haloarchaeal strains, designated S1BR25-6^T and S3BR25-2^T were classified within the genus *Halogeometricum* based on Overall Genome Related Indexes (OGRIs) such as Orthologous Average Nucleotide Identity, digital DNA-DNA hybridization, and Average Amino Acid Identity as standard criteria for species delineation. Moreover, this study embarks on an exhaustive genome-based comparative analysis of the haloarchaeal genus *Halogeometricum*, delineating the metabolic capacities, osmoregulatory adaptations, and resistance to certain heavy metals of its species. The dual osmoregulatory mechanism observed by *in-silico* analysis of the *Halogeometricum* species combines "salt-in" and "salt-out" strategies which highlights the adaptive flexibility of these haloarchaea. In addition, capability for *de novo* thiamine biosynthesis of strain S1BR25-6^T along with other *Halogeometricum* species underscores their metabolic complexity and resilience, offering insights into their role in ecosystem dynamics and potential biotechnological applications. Wet lab experimental analysis of strains S1BR25-6^T and S3BR25-2^T confirmed their resistance to heavy metals, particularly to arsenic, zinc, and cadmium, emphasizing their potential for bioremediation applications. Furthermore, conducting fragment recruitment analysis across different metagenomic datasets revealed a predominant recruitment of species from the genus *Halogeometricum* in hypersaline soils of Odiel Saltmarshes (especially the two novel strains), and in the brines of marine saltern ponds with high salt concentrations. These results contribute to a reinforced understanding of the extremely halophilic characteristics inherent to the genus *Halogeometricum*. Finally, taxogenomic analysis has substantiated that strains S1BR25-6^T (= CCM 9250^T = CECT 30624^T), and S3BR25-2^T (= CCM 9253^T = CECT 30622^T) denote two previously

unidentified species within the genus *Halogeometricum*, for which we propose the names *Halogeometricum salsisoli* sp. nov., and *Halogeometricum luteum* sp. nov., respectively.

KEYWORDS

haloarchaea, *Halogeometricum*, comparative genomic analysis, taxogenomics, thiamine biosynthesis, heavy metals

1 Introduction

Hypersaline environments are characterized by their high salt concentration, although other factors, such as temperature, pH or high concentrations of toxic compounds can also influence their microbiota (Rodríguez-Valera, 1988; Ventosa, 2006). Most hypersaline habitats are aquatic systems derived from seawater or salt deposits, such as marine salterns or saline lakes, and they are designated as thalassohaline ecosystems, showing relative salts contents similar to that of seawater but with higher values (Ventosa, 2006). Other saline habitats that have been less studied are saline and hypersaline soils. Despite their global presence and the growing salinization of soils due to irrigation and desertification, research into the microbial diversity within these areas remains limited, especially when compared to studies on saline lakes and marine salterns (Ventosa et al., 2008; Oren, 2011). Soil environments, as suggested by prior studies are the most diverse environments on Earth, presumptively due to the complex variability in soil structure and a greater frequency of disturbances (Vera-Gargallo and Ventosa, 2018; Vera-Gargallo et al., 2019). The soil microbiota is an indispensable component that supports the essential microbiological processes in soils. These processes include food supply, pharmaceutical development, carbon sequestration, pollution breakdown, climate moderation, and the nutrient cycles vital for sustaining higher forms of life (Bertola et al., 2021).

The predominant microbiota of hypersaline habitats is represented by extremely halophilic archaea, also designated as haloarchaea, as well as by halophilic bacteria belonging to a variety of phyla. Haloarchaea are currently classified within the class *Halobacteria*, divided into two orders, nine families and 82 genera (Cui et al., 2024). The genus *Halogeometricum* belongs to the family *Haloferacaceae*, within the order *Halobacteriales*, class *Halobacteria* and phylum *Methanobacteriota* (formerly "*Euryarchaeota*"). Currently, the genus *Halogeometricum* comprises four species. The type species, *Halogeometricum borinquense*, was isolated from the brine of a coastal marine solar saltern in Cabo Rojo, Puerto Rico, and described by Montalvo-Rodríguez et al. (1998). Later, Savage et al. (2008) described *Halosarcina pallida* BZ256^T, a sarcina-shaped strain isolated from a sulfide- and sulfur-rich spring in the USA. Eventually, it was transferred together with the species *Halosarcina limi*, isolated from a solar saltern in China (Cui et al., 2010a), to the genus *Halogeometricum*, as *Halogeometricum pallidum* and *Halogeometricum limi*, respectively (Qiu et al., 2013). Finally, *Halogeometricm rufum*, was isolated from a marine solar saltern in China (Cui et al., 2010b). Cells of species of this genus are extremely pleomorphic, aerobic and stain Gram-negative (Montalvo-Rodríguez et al., 1998). The polar lipids present in all members of this genus are phosphatidylglycerol (PG) and phosphatidylglycerol phosphate methyl ester (PGP-Me). Some species, additionally, possess a glycolipid chromatographically identical to sulfated diglycosil diether (S-DGD-1), as well as other minor glycolipids. An unsulfated glycolipid, designated "GLb", is the major polar lipid of *Halogeometricum borinquense* JCM 10706^T, which distinguishes it from the other species of this genus (Cui et al., 2010b; Qiu et al., 2013). Besides, phosphatidylglycerol sulfate (PGS) is not present in species of the genus *Halogeometricum*, in contrast to species of other related genera.

In this study, we performed a comprehensive genome-based comparative analysis of the genus *Halogeometricum*, focused on the metabolic functions, osmoregulatory strategies, and heavy metal adaptation mechanisms of its species. Among these, we paid exclusive attention to the thiamine biosynthesis pathways. Thiamine (vitamin B_1) is crucial for several key metabolic processes in cells across all domains of life. Its active form, thiamine diphosphate (ThDP), acts as a cofactor for enzymes that catalyze essential reactions in carbohydrate and amino acid metabolism, as well as in the synthesis of nucleic acids and neurotransmitters (Maupin-Furlow, 2018; Dhir et al., 2019). Vitamin B_1 possesses antioxidant, antimicrobial, and anti-inflammatory properties, alongside its well-established nutritional benefits, which suggest its potential use in food preservation (Taskiran and Ergul, 2021; Hsouna et al., 2022). It supports nervous and cardiovascular systems, increases the immunity system, enhances cognitive functions, aids digestion, and maintains muscle tone (Mrowicka et al., 2023). Thiamine deficiency can lead to serious health issues, such as Beriberi (Wilson, 2020), Wernicke–Korsakoff Syndrome (Isenberg-Grzeda et al., 2012), Leigh Syndrome (Ortigoza-Escobar et al., 2016), and others. The ability to *de novo* synthesize thiamine (vitamin B_1) is confined to bacteria, archaea, yeasts, and plants. Animals, including humans, are incapable of synthesizing thiamine due to the absence of the necessary enzymes, thereby requiring its intake through diet.

Furthermore, we conducted a pan-genome analysis of *Halogeometricum* species and assessed metagenomic fragment recruitment in various hypersaline environments in order to determine the presence and/or abundance of species of this genus in different saline habitats. With the aim to isolate new halophilic taxa, a culturomics approach was carried out and two strains related to the genus *Halogeometricum* were isolated. We have characterized these two new haloarchaeal strains isolated from the Odiel Saltmarshes, and we propose them as new species of the genus *Halogeometricum*.

2 Materials and methods

2.1 Samples analysis and strains isolation and cultivation

We conducted a sampling in the Odiel Saltmarshes, a marine-influenced natural area of tidal wetlands located at the estuary of the Odiel and Tinto rivers at the confluence of the Atlantic Ocean, in Southwestern Spain. The selected sampling sites were located in a plant-free high marsh zone, predominantly influenced by rainfall as the main water source, although subjected to inundation during periods of high tides (Grande et al., 2003). The sampling was carried out in July 2020, during a period unaffected by flooding, enabling the collection of samples from the hypersaline soils within this area. Several physico-chemical characteristics of the samples were determined. The pH and electrical conductivity were determined with a pH meter (CRISON BASIC 20) and a conductometer (CRISON 35+), respectively, after a 1:2.5 dilution of the sample. Other features of two soil samples, designated as 1B (37°12'26.6"N 6°57'52.5"W) and 3B (37°13'18.0"N 6°57'44.8"W), corresponding to the isolation places of the studied strains, included the presence of heavy metals, texture and organic matter, and were analyzed by Innoagral Laboratories, in Brenes (Sevilla, Spain).

Strains S1BR25-6^T and S3BR25-2^T were isolated in pure culture after serial dilutions and plating under sterile conditions and incubation at 37°C for up to 3 months. We used Reasoner's 2A (R2A) medium (Difco) as an isolation and cultivation medium supplemented with 25% (w/v) seawater salt solution prepared by dilution of 30% (w/v) stock solution (Subov, 1931) (designated as R2A 25 medium), which is composed of (g l^{-1}): NaCl, 195; $MgCl_2{\cdot}6H_2O$, 32.5; $MgSO_4{\cdot}7H_2O$, 50.8; $CaCl_2$, 0.83; KCl, 5.0; $NaHCO_3$, 0.17; NaBr, 0.58. The pH of the medium was adjusted to 7.5 with 1 M KOH and purified agar was added to a final concentration of 2% (w/v) to prepare the solid media. Cultures were preserved at -80°C in R2A 25 (w/v) liquid medium containing 40% (v/v) glycerol.

2.2 DNA extraction, amplification and sequencing

To extract the genomic DNA of strains S1BR25-6^T and S3BR25-2^T, the methodology described by Marmur (1961) modified for small volumes was followed. The PCR was carried out using a Bio-Rad T100 Thermal Cycler to amplify the 16S rRNA and *rpoB'* genes. The universal archaeal primers ArchF and ArchR (DeLong, 1992; Arahal et al., 1996) were used to target 16S rRNA gene and rpoBF and rpoBR primers for *rpoB'* gene amplification (Fullmer et al., 2014). To purify both, genomic DNA and PCR products, MEGAquick-spin™ Plus Fragment DNA Purification Kit (iNtRON Biotechnology) was used following the manufacturer's protocol. DNA concentration was examined fluorometrically with Qubit 4 Fluorometer (Thermo Fisher Scientific), and the quality was checked with NanoDrop One Spectrophotometer (Thermo Fisher Scientific). Stab Vida (Caparica, Portugal) sequenced the PCR amplicons using the Sanger method. The whole genome sequencing of strains S1BR25-6^T and S3BR25-2^T was provided by Novogene Europe (Cambridge, United Kingdom) using the Illumina (San Diego, CA, USA) NovaSeq 6000 platform, following a 2 × 150-bp paired-end strategy.

2.3 Phylogenetic and taxogenomic analysis

The 16S rRNA and *rpoB'* gene sequences of the two isolated strains were assembled with ChromasPro software v.1.5 (Technelysium Pty Ltd., Brisbane, Australia), and phylogenetically identified by comparing with the sequences available in the EzBioCloud database (Yoon et al., 2017) and NCBI GenBank database by BLASTN search (Altschul et al., 1990). ARB Tool Fast aligner v.7.0 (Ludwig et al., 2004) and BioEdit program v.3.3.19.0 (Alzohairy, 2011) enabled to obtain the complete multiple sequence alignments corresponding to the 16S rRNA and *rpoB'* genes, respectively. The phylogenetic treeing based on 16S rRNA and *rpoB'* gene sequence data was carried out using the ARB software v.7.0 (Ludwig et al., 2004). Phylogenetic tree reconstructions were conducted using the maximum-likelihood (Felsenstein, 1981), neighbor-joining (Saitou and Nei, 1987), and maximum-parsimony algorithms (Felsenstein, 1983). The "gitana" script (Galisteo, 2022) was used for formatting and visualization of the phylogenetic trees. The 16S rRNA and *rpoB'* gene sequences of strains S1BR25-6^T and S3BR25-2^T were deposited in GenBank/EMBL/DDBJ, under the accession numbers ON653036 and ON682483 (16S rRNA gene), and ON668042 and ON668043 (*rpoB'* gene), respectively.

The recommendations regarding the quality of genomic sequences and the criteria for their use in taxogenomic studies were followed (Chun et al., 2018; Riesco and Trujillo, 2024). The genome reads of strains S1BR25-6^T and S3BR25-2^T were assembled by k-mer approach using Spades v.3.13.0 (Prjibelski et al., 2020). Completeness and contamination of the assemblies were verified by CheckM v1.0.5 (Parks et al., 2015). The standard annotation was carried out by Prokka v.1.12 (Seemann, 2014) and followed by the recovery of the 16S rRNA and *rpoB'* gene sequences from the genome to verify their compliance with the genuine Sanger sequences. The genome sequences of the studied strains, together with the genomes of related strains of the genus *Halogeometricum*, and those of closely related taxa of the family *Haloferacaceae* available in the NCBI GenBank database, were used to establish phylogenomic relationships between species. The open reading frames of the

coding sequences (CDS) were extracted from the genomes using Prodigal v. 2.60 (Hyatt et al., 2010). Among all the CDS extracted, those corresponding to single-copy orthologous protein set and present in all the genomes were identified using scripts from the Enveomics package (Rodríguez-R and Konstantinidis, 2016) and further aligned using Muscle v.5.1 (Edgar, 2022). FastTreeMP v.2.1.8 (Price et al., 2010) was used to reconstruct an approximately maximum-likelihood phylogenomic tree based on 848 single-copy core-orthologous protein sequences. The whole-genome sequences of strains S1BR25-6^T and S3BR25-2^T were deposited in GenBank/EMBL/DDBJ, under the accession numbers JAMQOP000000000 and JAMQOQ000000000, respectively.

2.4 Comparative genomic analysis

To confirm the taxonomic affiliation of the studied strains, the Overall Genome Relatedness Indexes (OGRIs) were calculated. Specifically, the Orthologous Average Nucleotide Identity (OrthoANI), the digital DNA-DNA hybridization (dDDH), and the Average Amino acid Identity (AAI) were obtained through OrthoANIu tool v.1.2 (Lee et al., 2016), the Genome-to-Genome Distance Calculator (GGDC) v.3.0 from the Leibniz Institute DSMZ (Braunschweig, Germany) (Meier-Kolthoff et al., 2022), and the 'aai.rb' script from the Enveomics collection (Rodríguez-R and Konstantinidis, 2016), respectively.

Furthermore, the Enveomics tool was used to carry out a pan-genome analysis (Rodríguez-R and Konstantinidis, 2016). Visualization of the pan-genome was conducted using the Anvi'o tool v.7 (Eren et al., 2015). To depict the core, variable ("shell"), and strain-specific genes, a flower plot was generated through the 'plotrix' package v.3.8.2 in R. Graphical representations showing the evolution of both the pan-genome and core-genome within the genus *Halogeometricum* were illustrated using the Pan-Genome Profile Analyze Tool (PanGP) v.1.0.1 (Zhao et al., 2014). Additionally, a heatmap based on the gene presence/absence within the variable genome was created using the 'gplot' R package v.3.1.3. The assignment of KO numbers to the genomes orthologous genes and their subsequent mapping to KEGG pathways and modules for reconstructing metabolic pathways were conducted using BlastKOALA functional annotation tool v.3.0 (Kanehisa et al., 2016). The circular genome maps of strains S1BR25-6^T and S3BR25 were generated with DNAPlotter v.18.2.0 (Carver et al., 2009). Furthermore, the identification of CRISPR-Cas systems was carried out using the CRISPRCasFinder tool v.4.2.21 (Couvin et al., 2018). In addition, isoelectric points of predicted proteomes were calculated by the 'iep' program of the EMBOSS package v.6.5.7.0 (Rice et al., 2000).

2.5 Phenotypic and chemotaxonomic characterization

Phenotypic features of strains S1BR25-6^T and S3BR25-2^T were determined according to the minimal standards for the description of new taxa of the class *Halobacteria* (Cui et al., 2024). To determine cell morphology and motility of the studied strains, they were grown on R2A 25 medium on a shaking incubator at 200 rpm at 37°C and the cells were observed by a light phase-contrast microscope (Zeiss Axioscope 5). Gram staining was performed as described by Dussault (1955). To determine the optimal salt requirements, the strains were cultured in R2A medium with different salt concentrations (0.5, 5, 7.5, 10, 12, 15, 17, 20, 22, 25, and 30% [w/v]). The pH range for the growth was determined in R2A 25 buffered medium adjusted to pH values from 5.0 to 9.5 (at 0.5 pH unit intervals). The temperature range for growth was examined by incubation in R2A 25 medium at 20°C to 55°C (at intervals of 5°C). Catalase activity was observed by adding a few drops of 3% H_2O_2 (v/v) to a young culture of the microorganisms (Cowan and Steel, 1993). The oxidase test was conducted by using 1% (v/v) tetramethyl-*p*-phenylenediamine (Kovács, 1956). R2A 25 medium plates supplemented with three alternative electron acceptors (DMSO, KNO_3, and L-arginine) were incubated at 37°C for 14 days in a GasPak system using AnaeroGen (Oxoid) to detect whether strains S1BR25-6^T and S3BR25-2^T were able to grow anaerobically. Biochemical and nutritional characterization was carried out following the methodology previously described by Straková et al. (2024). *Halogeometricum borinquense* DSM 11551^T was used as a reference strain for phenotypic feature comparison.

Determination of polar lipids has proved to be a useful marker in the characterization and delimitation of haloarchaea at the genus level (Torreblanca et al., 1986; Oren et al., 1997; Cui et al., 2024). The polar lipids were extracted from a cell biomass of the studied strains S1BR25-6^T and S3BR25-2^T and from the reference strains *Halobacterium salinarum* DSM 3754^T, *Halorubrum saccharovorum* DSM 1137^T, and *Halogeometricum borinquense* DSM 11551^T by using a chloroform/methanol system. The identification of polar lipid profiles was carried out by high-performance thin-layer chromatography (HPTLC) on silica gel glass plates (Merck) developed in chloroform–methanol–90% acetic acid (39.4/2.42/18.18 mL) solvent system. The polar lipids were revealed by 5% (v/v) sulfuric acid followed by heating at 160°C and, in addition, phospholipids were specifically detected by molybdenum blue spray reagent (Angelini et al., 2012; Corral et al., 2013).

2.6 Determination of minimum inhibitory concentrations for heavy metals

Susceptibility to selected heavy metals (copper, cadmium, zinc, lead, and arsenic) was tested for the two novel strains. Cultures of strains S1BR25-6^T and S3BR25-2^T, incubated for 7 days in R2A 25 medium, were used to inoculate Petri dishes containing R2A 25 agar medium with varying concentrations (0.01, 0.05, 0.5, 1, 2.5, 4, 5, 10, 20, 50, 80, 100, 150, 200, 300, 500, 600, and 700 mM) of heavy metal salts: $CuSO_4$, $CdCl_2 \cdot H_2O$, $ZnSO_4 \cdot 7H_2O$, $Pb(C_2H_3O_2)_2 \cdot 3H_2O$, and $C_2H_6AsNaO_2 \cdot 3H_2O$. The heavy metal solutions were sterilized by filter membrane (pore size of 0.2 µm) before being added to the culture medium. After incubation at 37°C for 1 to 4 weeks, the tolerance of the colonies to each heavy metal was evaluated. The minimum concentration of each heavy metal that completely inhibited haloarchaeal growth was identified as the minimum

inhibitory concentration (MIC). R2A 25 agar media without any heavy metals served as controls for each isolate.

2.7 Metagenomic fragment recruitment analyses

Analysis of metagenomic reads recruitment was conducted using seven environmental metagenomic datasets (Supplementary Table S1) with the aim to detect and quantify the presence of the four *Halogeometricum* species, along with strains S1BR25-6^T and S3BR25-2^T, across diverse aquatic and terrestrial saline habitats. Reference genomes of *Haloquadratum walsbyi* C23^T (GCF_000237865.1) and *Spiribacter salinus* M19-40^T (GCF_000319575.2) were included for comparative purposes. To mitigate analysis bias, contigs from each genome sequence were concatenated and, subsequently, rRNA gene sequences were masked. A BLASTN search was employed with specific parameters (alignment length ≥ 30 nt, similarity > 95%, E-value ≤ 10^{-5}) to map quality-filtered metagenomic reads against each genome. Recruitment plot representations were generated using the 'Hmisc' library v.5.1.0 in R.

3 Results and discussion

3.1 Odiel saltmarshes samples composition reveals increased levels of certain heavy metals

Two saline soil samples (designated 1B and 3B) from Odiel Saltmarshes (Huelva), at the confluence of the rivers Odiel and Tinto with the Atlantic Ocean were examined. The pH and the electrical conductivity of the soil sample 1B, from which strain S1BR25-6^T was isolated, were 7.9 and 98.5 mS/cm, respectively. The soil sample 3B, corresponding to the isolation place of strain S3BR25-2^T, presented a pH value of 6.5 and an electrical conductivity of 202.0 mS/cm. Both soils can be considered as hypersaline, with electrical conductivities much higher than 4 mS/cm, a limit suggested for saline soils (Richards, 1954). The hypersaline soil samples were analytically tested for the presence of heavy metals (Supplementary Table S2) due to their possible contamination as a consequence of the past metallurgic operations in this area. Concentrations of certain prevalent heavy metals such as copper and lead of both studied soil samples and cadmium in 1B soil sample were high but found to be in accordance with the given standards of uncontaminated soils designated by the Environment Department of the regional Government of Andalusia (Consejería de Medio Ambiente, 1999). Yet, arsenic and zinc concentrations of the tested soil samples exceeded the reference intervals, which suggest a certain heavy metal tolerance or/and resistance of the two isolated strains. Haloarchaeal representatives have demonstrated significant capacity in resistance to toxic heavy metals (Krzmarzick et al., 2018; Vera-Bernal and Martínez-Espinosa, 2021; Tavoosi et al., 2023), however further investigation should be carried out.

3.2 Two newly discovered species within the genus *Halogeometricum* through phylogenetic and phylogenomic analysis

Based on the 16S rRNA gene sequence identities, strains S1BR25-6^T and S3BR25-2^T were most closely related to *Halogeometricum pallidum* BZ256^T (99.3% and 99.1%), *Halogeometricum rufum* RO1-4^T (98.4% and 98.3%), *Halogeometricum limi* RO1-6^T (98.4 and 97.5%), and *Halogeometricum borinquense* PR3^T (97.6% and 97.3%), respectively. Analysis of the *rpoB'* gene sequences also showed the closest relatedness of isolates S1BR25-6^T and S3BR25-2^T to *Halogeometricum pallidum* JCM 14848^T (94.9% and 95.6%), *Halogeometricum rufum* CGMCC 1.7736^T (92.1% and 92.0%), *Halogeometricum limi* CGMCC 1.8711^T (90.8 and 91.1%), and *Halogeometricum borinquense* ATCC 700274^T (89.0% and 89.0%), respectively. The identity between the two studied strains based on their 16S rRNA gene sequences was 99.84%, and 96.18% based on their *rpoB'* gene sequences. The topology of the phylogenetic trees based on the 16S rRNA (Supplementary Figure S1) and the *rpoB'* (Supplementary Figure S2) gene sequences confirmed the affiliation of the two studied strains to the genus *Halogeometricum*.

The main genome features of strains S1BR25-6^T, S3BR25-2^T and other type strains of the species within *Halogeometricum* are shown in Supplementary Table S3. The phylogenomic tree reconstruction, based on the comparison of 848 single-copy core-orthologous proteins, showed that the studied strains clustered together within the genus *Halogeometricum*, but far enough from the already described species of this genus, and thus, supporting their affiliation as two novel species (Figure 1).

3.3 Comparative genomic analysis: unraveling evolutionary relationships and genome dynamics

The genomes of the two studied strains and those of the type strains of the related species available in the GenBank database were used to estimate the OGRIs among the species of the family *Haloferacaceae*. The comparative analysis of the genomic identity revealed that the two new isolates exhibited percentages ranging 89.0–79.3% (OrthoANI), 36.9–22.9% (dDDH), and 89.1–75.5% (AAI) when compared to *Halogeometricum* species. OrthoANI and dDDH values between strains S1BR25-6^T and S3BR25-2^T were 90.7% and 41.0%, respectively (Figure 2), confirming unequivocally that these two strains represent two different species according to the accepted threshold values for prokaryotic species delineation: 95–96% for OrthoANI and 70% for dDDH (Goris et al., 2007; Richter and Rossello-Mora, 2009; Auch et al., 2010; Chun and Rainey, 2014; Cui et al., 2024). AAI values between strains S1BR25-6^T and S3BR25-2^T and the species of the genus *Halogeometricum* varied from 89.1 to 75.5%, and AAI value between the two studied strains was 90.6%, providing further evidence that strains S1BR25-6^T and S3BR25-2^T should be classified within the genus *Halogeometricum* as two different novel species (Figure 3).

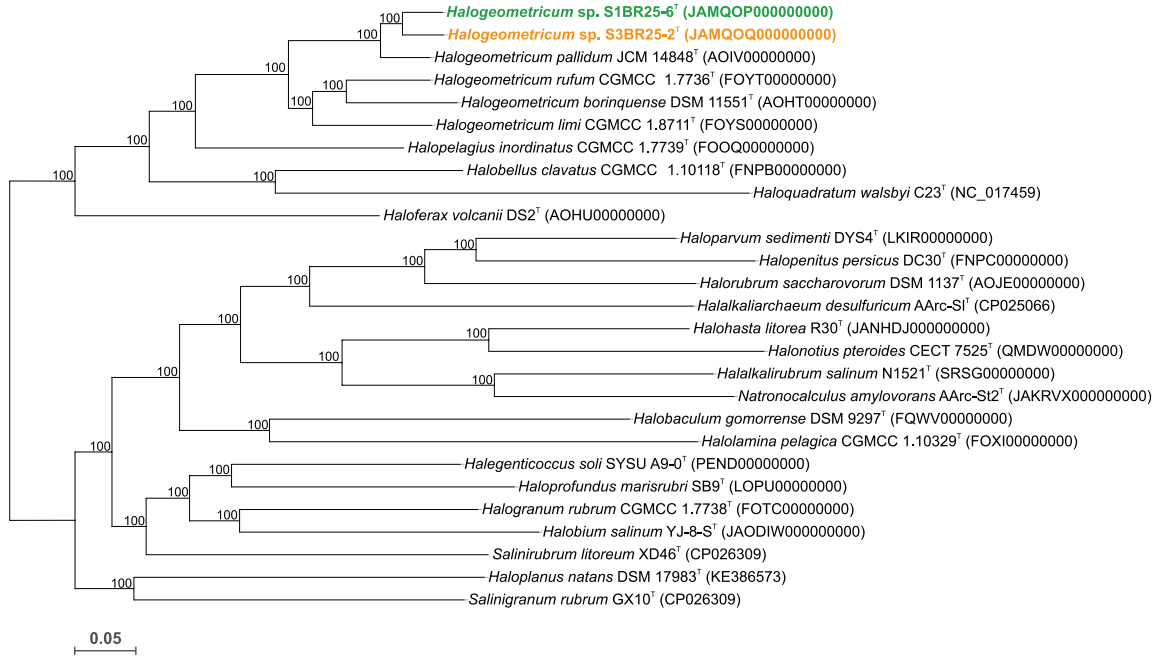

FIGURE 1
Approximate maximum-likelihood phylogenomic tree based on the comparison of 848 single-copy core-orthologous proteins showing the relationships between strains S1BR25-6^T, S3BR25-2^T, members of the genus *Halogeometricum*, and other related species within the family *Haloferacaceae*. Sequence accession numbers are shown in parentheses. Branch support values (%) are computed with the Shimodaira-Hasegawa test and are shown at branch points. Bar, 0.05 substitutions per amino acid position.

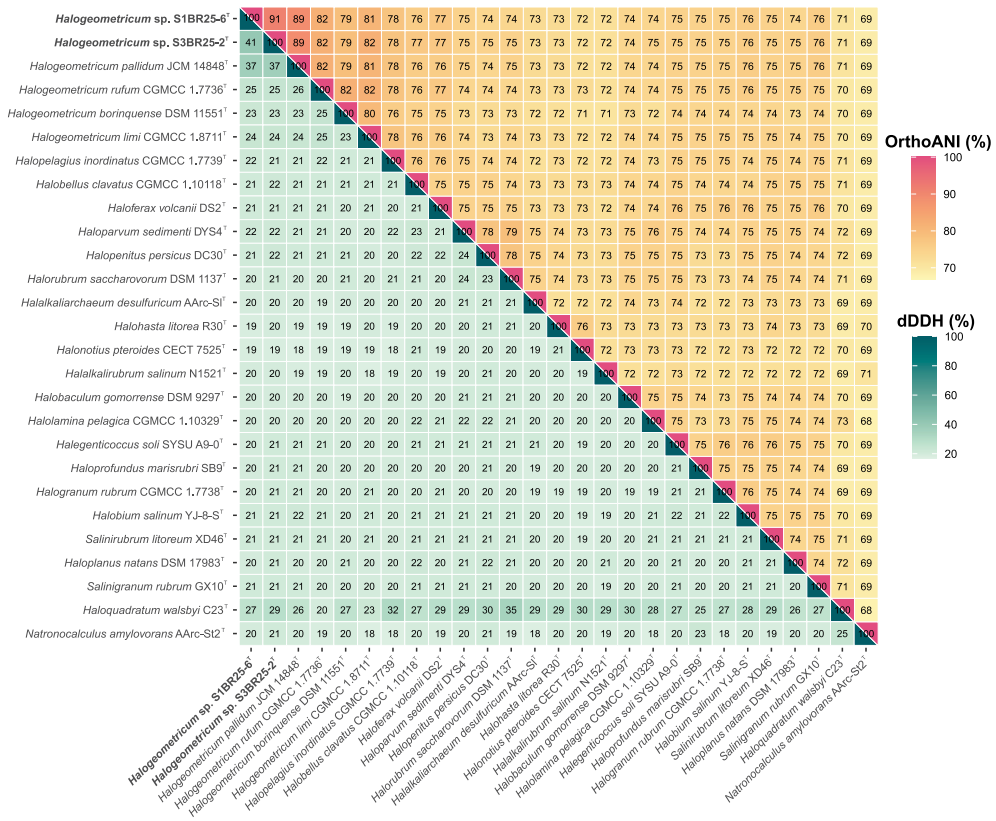

FIGURE 2
Heatmap displaying Orthologous Average Nucleotide Identity (OrthoANI) (upper right) and digital DNA-DNA hybridization (dDDH) (lower left) percentages among strains S1BR25-6^T and S3BR25-2^T, members of the genus *Halogeometricum*, and other related species of the family *Haloferacaceae*.

The pan-genome of prokaryotes consists of three gene categories: core, variable (also denoted as "shell", shared by some but not all the strains), and singleton (also designated as "cloud", strain-specific) gene clusters (Tettelin et al., 2005). We analyzed nine genomes of the genus *Halogeometricum*, including the two novel strains S1BR25-6^T and S3BR25-2^T, the four type strains of the current species of the genus (*Halogeometricum borinquense* DSM 11551^T, *Halogeometricum limi* CGMCC 1.8711^T, *Halogeometricum pallidum* JCM 14848^T, and *Halogeometricum rufum* CGMCC 1.7736^T), and three non-type reference strains (*Halogeometricum borinquense* wsp4 [GCA_010692885.1], *Halogeometricum borinquense* N11 [GCA_004150395.1], and *Halogeometricum* sp. CBA1124 [GCA_009741955.1]). Within the nine analyzed genomes of the genus *Halogeometricum*, 37,306 translated CDSs were identified and categorized into 5,921 orthologous gene clusters (OGs), consisting of 1,977 core OGs and 3,944 variable ones. Additionally, 3,496 singletons gene clusters were identified, forming a pan-genome comprising a total of 9,417 gene clusters (Figure 4). The evolutionary dynamics of pan-genome and core-genome sizes (Figure 5) depict changes in the overall gene repertoire (pan-genome) and the collection of shared genes (core-genome) within the genus *Halogeometricum* across evolutionary time. The pangenome of the species of the genus *Halogeometricum* is considered open, as the continual addition of new genomes introduces novel genes, reflecting ongoing evolutionary processes. This open nature of the pan-genome highlights the genomic plasticity and adaptability of *Halogeometricum* species to diverse and extreme environments. In contrast, the core genome is considered closed, as its size remains relatively stable over time. Figure 6 represents a visual representation of a binary matrix illustrating the occurrence (presence or absence) of variable genes within the family *Haloferacaceae*. The unique clusters of variable genes associated with each genus offer a glimpse into the genomic diversity within the microbial community of the family *Haloferacaceae*. Additionally, with 418 and 686 strain-specific gene clusters, respectively, the studied strains show distinct genomic profiles, reinforcing the previous conclusion that they both represent unique, previously unidentified species.

3.4 Phenotypic and chemotaxonomic features confirm the unique identity of the new species and their affiliation to the genus *Halogeometriucum*

We carried out a complete phenotypic characterization of the two new strains, which involved morphological, physiological, biochemical, and nutritional characterization. The summary of

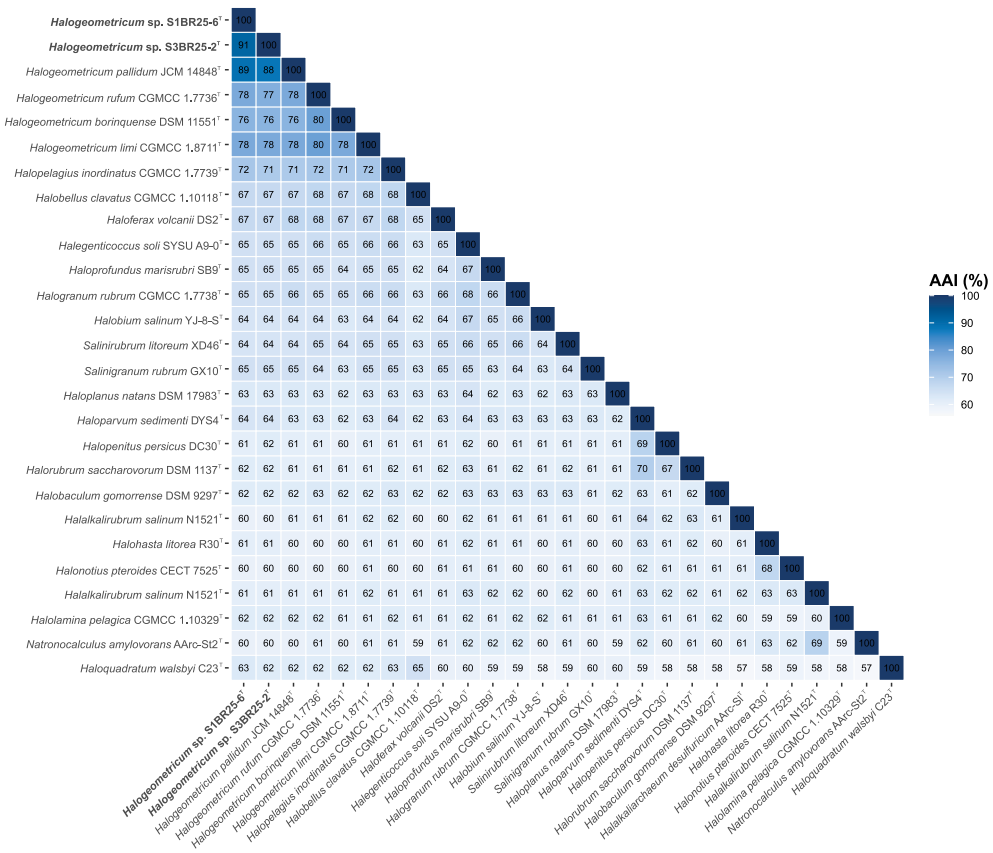

FIGURE 3
Heatmap showing Average Amino acid Identity (AAI) percentages among *Halogeometricum* species, including strains S1BR25-6^T and S3BR25-2^T, and other related species of the family *Haloferacaceae*.

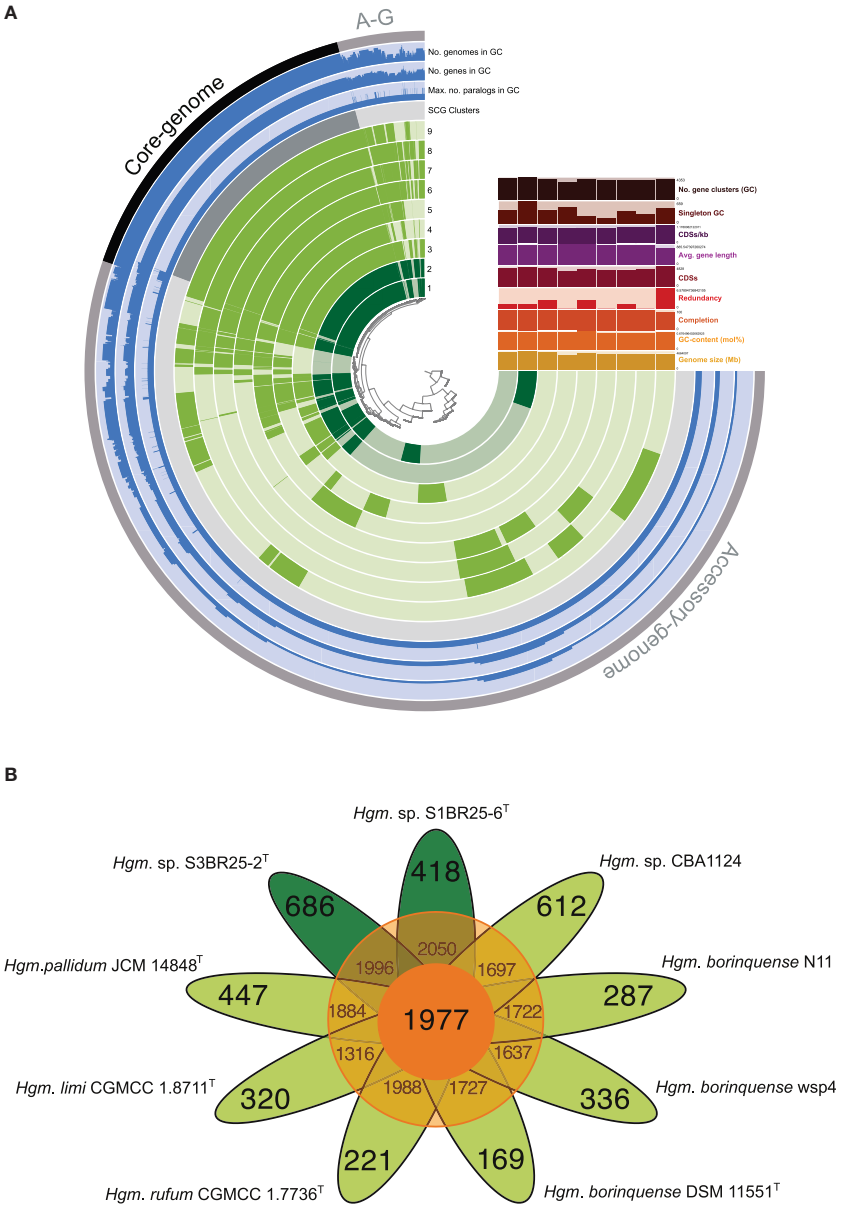

FIGURE 4
(A) A comparative pan-genome analysis among the nine *Halogeometricum* strains: 1. Strain S1BR25-6^T; 2. Strain S3BR25-2^T; 3. *Halogeometricum pallidum* JCM 14848^T; 4. *Halogeometricum limi* CGMCC 1.8711^T; 5. *Halogeometricum rufum* CGMCC 1.7736^T; 6. *Halogeometricum borinquense* DSM 11551^T; 7. *Halogeometricum borinquense* wsp4; 8. *Halogeometricum borinquense* N11; 9. *Halogeometricum* sp. CBA1124. In the layers, dark colors indicate the presence of a gene cluster and light colors indicate its absence. **(B)** Flower plot showing the core (in the center), variable (in the annulus), and strain-specific (in the petals) genes of the nine *Halogeometricum* strains.

the phenotypic characteristics is shown in Supplementary Table S4 and in the new species descriptions included in the conclusion section. The phenotypic features of the new isolates agree with those described for the species of the genus *Halogeometricum* and, at the same time, they allow distinguishing the new proposed taxa. Particularly, strains S1BR25-6^T and S3BR25-2^T differed in their cell morphology, colony pigmentation, and utilization of acetate, dulcitol, fumarate, lactose, mannitol, and L-arginine. Unlike the other four already described species of *Halogeometricum*, the two new proposed species were unable to utilize glutamate as a sole carbon and energy source.

The HPTLC analysis revealed that strains S1BR25-6^T and S3BR25-2^T possessed the following polar lipids: phosphatidylglycerol (PG), phosphatidylglycerol phosphate methyl ester (PGP-Me), and a glycolipid chromatographically identical to sulfated diglycosyl diether (S-DGD-1) (Supplementary Figure S3). Traces of biphosphatidylglycerol (BPG) and minor unidentified glycolipids were also present. Phosphatidylglycerol sulfate (PGS) was not present in either of the two studied strains. The lipid profiles of strains S1BR25-6^T and S3BR25-2^T are in concordance with the lipid profiles described for species of the genus *Halogeometricum* (Montalvo-Rodriguez et al., 1998; Cui et al., 2010b).

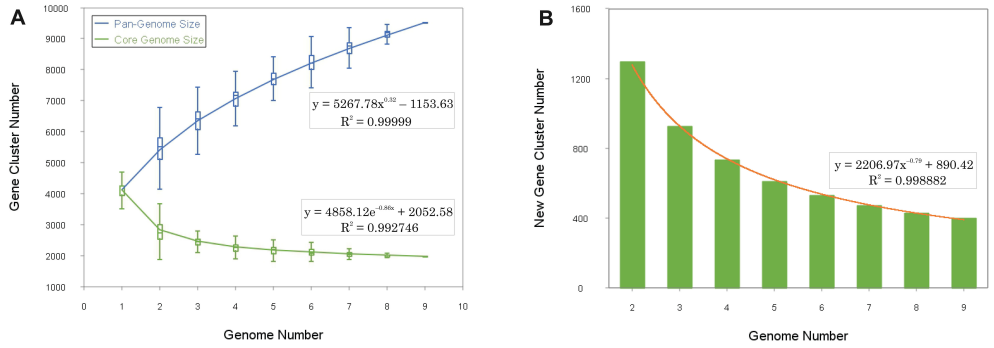

FIGURE 5
Gene accumulation curves of the pan-genome (blue) and the core-genome (green) of representatives of the genus *Halogeometricum* **(A)**, with the curve representing the least squares fit of the power law for average values **(B)**.

3.5 Habitat distribution patterns of the genus *Halogeometricum*

We conducted a metagenomic fragment recruitment analysis to investigate the distribution and abundance of DNA fragments associated with the two novel species, represented by strains S1BR25-6^T and S3BR25-2^T, as well as other species of the genus *Halogeometricum*. Supplementary Figure S4 shows the recruitments of strains S1BR25-6^T and S3BR25-2^T against seven metagenomic databases sourced from marine-derived environments: hypersaline soils in Huelva (SMO1 and SMO2) (Vera-Gargallo et al., 2018), the brines of four ponds in Santa Pola salterns with varying salinities ranging from 13% to 37% (SS13, SS19, SS33, SS37) (Fernández et al., 2014; Ghai et al., 2011), and Gujarat saline desert (Patel et al., 2015). Particularly abundant recruitments were observed in the hypersaline soils of Odiel Saltmarshes in Huelva, predominantly represented by the two studied strains, S1BR25-6^T and S3BR25-2^T, which were isolated from this saline habitat. This was followed by the ponds of the Santa Pola salterns with 33% and 37% (w/v) salt concentrations, respectively (Figure 7). Lower recruitment values were noted at lower salt concentrations, confirming the distinctly extremely halophilic nature of the species within the genus *Halogeometricum*.

3.6 Metabolic strategies: a genomic perspective

The primary metabolic pathways of the species of the genus *Halogeometricum* were mapped through the analysis of their genomes using the BlastKOALA tool for annotation and the most frequently occurring metabolic pathways are shown in Figure 8. The key orthologs involved in the central carbohydrate metabolism were present in all genomes of *Halogeometricum* members, highlighting their heterotrophic metabolic potential. The conversion of pyruvate to acetyl-CoA, through both aerobic and anaerobic pathways using pyruvate dehydrogenase and pyruvate ferredoxin oxidoreductase, respectively, was observed (Supplementary Figure S5). Moreover, the genomes of *Halogeometricum limi* CGMCC 1.8711^T, *Halogeometricum pallidum* JCM 14848^T, and the two new strains, S1BR25-6^T and S3BR25-2^T, contained genes involved in the assimilation of nitrate (Supplementary Figure S5), initially reducing nitrate to nitrite, followed by the conversion of nitrite to ammonia. Furthermore, all four species possessed nitrate/nitrite transporters. On the contrary, genes associated with the denitrification process have been only found in *Halogeometricum borinquense* DSM 11551^T and *Halogeometricum rufum* CGMCC 1.7736^T. In addition, genes that encode enzymes capable of catalyzing the conversion of nitroalkane to nitrite in *Halogeometricum rufum* CGMCC 1.7736^T and formamide to ammonia in strains S1BR25-6^T and S3BR25-2^T have been identified. All six members of the *Halogeometricum* genus possessed the ammonia transporter, as well as glutamine synthetase and glutamate synthase, that are essential for nitrogen metabolism. Moreover, the genomes revealed the complete biosynthesis pathways for several amino acids, including arginine, cysteine, histidine, isoleucine, leucine, threonine, tryptophan, and valine (Supplementary Figure S5). ABC transporters for saccharides, phosphates, amino acids, mineral and organic ions, and metals were abundant in the genomes under study. The ATP-dependent phosphate uptake transporter (pstSCAB) was encoded across all *Halogeometricum* genomes (Supplementary Figure S5). Moreover, *Halogeometricum borinquense* DSM 11551^T, *Halogeometricum limi* CGMCC 1.8711^T, and *Halogeometricum rufum* CGMCC 1.7736^T possessed genes encoding for an additional phosphonate uptake transporter (phnCDE). Regarding the transport of biologically essential magnesium ions, genes for MgtE and MgtE-like Mg^{2+} channels were identified. ABC transporters responsible for the uptake of zinc, cobalt, copper, iron, sulfonate, molybdate, tungstate, spermidine, putrescine, etc. were also found within the *Halogeometricum* genomes (Supplementary Figure S5). The studied genomes also possessed functional orthologs associated with the biosynthesis and metabolism of cofactors and vitamins, including folate, pantothenate, and Coenzyme A, as well as the metabolism of nicotinate and nicotinamide, biotin, and thiamine (Supplementary Figure S5).

In addition, we delved into the functional genomic analysis targeting the distinct characteristics of the new strains as identified through phenotypic characterization (section 3.4). The genomic annotation of both strains regarding the utilization of glutamate and lactose as sole carbon and energy sources was consistent with the findings from the phenotypic study. The two strains possessed genes for glutamate dehydrogenase, which is involved in glutamate deamination. However, they lacked genes for glutamate transporters

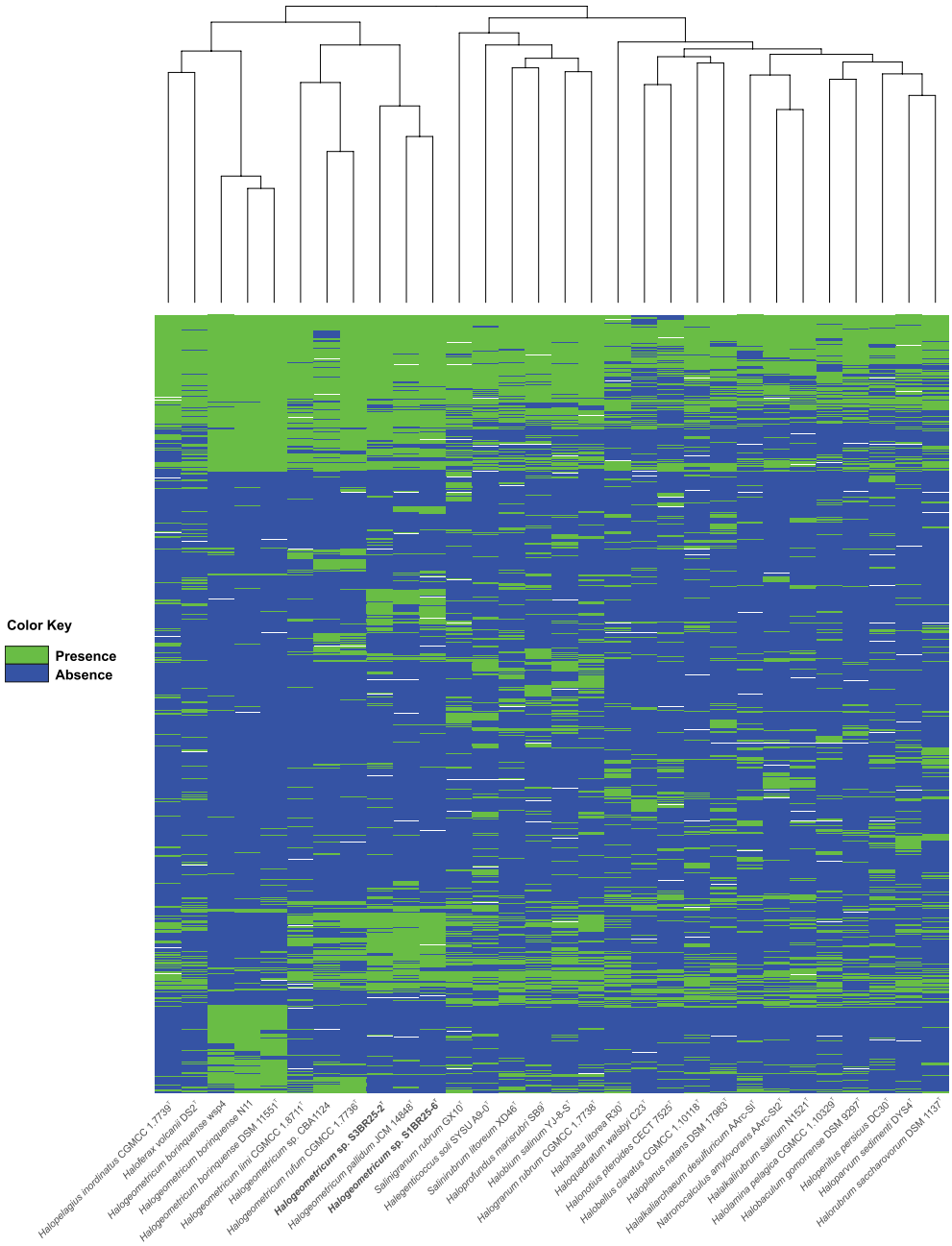

FIGURE 6
Heatmap based on the presence/absence of the variable orthologous gene clusters within the *Haloferacaceae* family. Each row corresponds to an orthologous gene cluster and each column corresponds to a strain. The green color represents the presence of the gene while the blue color represents its absence.

such as GltT, GltP, GltS, GadC, GlnPQ, GlnHMPQ, and DctA, which prevented the uptake and utilization of glutamate (Supplementary Figure S5). The ability to utilize lactose was confirmed in strain S1BR25-6^T. The *ebgA* gene, encoding the enzyme evolved β-galactosidase (EbgA), which hydrolyzes β-galactosides such as lactose into monosaccharides, was identified in that strain. The *ebg* operon can adapt through mutations to enhance its function, allowing it to compensate for the lack of *lacZ* gene (also encoding a β-galactosidase) and to support growth on lactose (Hall, 1982; Hall et al., 1989). Moreover, strain S1BR25-6^T contained LacEFG transport system responsible for the uptake and phosphorylation of lactose (Supplementary Figure S5). On the other hand, strain S3BR25-2^T lacked both the enzyme and transporters necessary for lactose utilization, which aligns with the results from the phenotypic study. The functional genomic analysis of strain S1BR25-6^T corroborated the phenotypic findings related to the utilization of substrates such as acetate, fumarate, dulcitol, and mannitol. The strain contained genes encoding the relevant enzymes and transporters, including acetyl-CoA

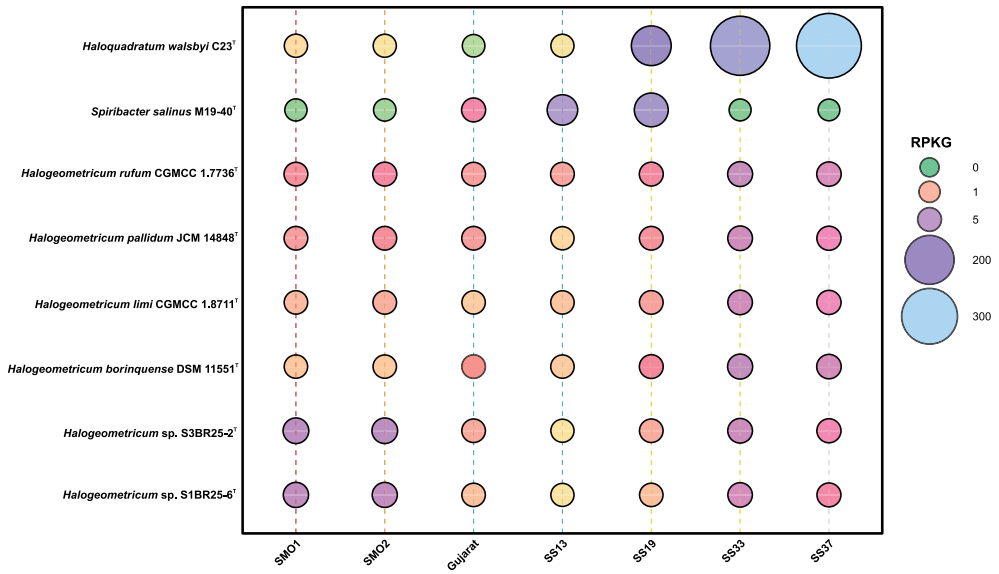

FIGURE 7
Bubble chart of relative abundance represented as RPKG (reads recruited per kilobase of genome per gigabase of metagenome) of strains S1BR25-6^T and S3BR25-2^T, the species of the genus *Halogeometricum*, and two reference species, namely, the haloarchaeon *Haloquadratum walsbyi* and the bacterial species *Spiribacter salinus*, within different metagenomic datasets (Supplementary Table S1).

synthetase (Acs) and AtoE transporter for acetate utilization, as well as fumarate reductase (Frd) and sodium dicarboxylate symporters (SdcS) for fumarate metabolism (Supplementary Figure S5). Conversely, the genes associated with dulcitol and mannitol metabolism were not annotated. Strains S1BR25-6^T and S3BR25-2^T both possessed genes encoding arginase, which converts arginine into ornithine and urea, as well as the ArcD transporter and ArcR regulatory protein (Supplementary Figure S5). However, only strain S3BR25-2^T showed growth in the presence of arginine in the phenotypic study. Additionally, the genome of strain S3BR25-2^T encoded acetyl-CoA synthetase (Acs), AtoE transporter, fumarate reductase (Frd), and sodium dicarboxylate symporters (SdcS) (Supplementary Figure S5). Despite this, the strain S3BR25-2^T did not exhibit growth on acetate and fumarate in the phenotypic study. This discrepancy might be due to inadequate expression of the genes encoding those enzymes and transporters. Regulatory mechanisms may require specific environmental signals or inducers absent in laboratory conditions. Moreover, strain S3BR25-2^T demonstrated growth in the presence of dulcitol and mannitol in the phenotypic study, even though relevant genes were not annotated in its genome. This could be attributed to cross-specificity of existing transporters, uncharacterized genes, alternative metabolic pathways, enzyme promiscuity, environmental adaptation, or potential gene misannotation. Furthermore, both novel strains contained genes encoding carotenoid 3,4-desaturase (CrtD), a bifunctional lycopene elongase/1,2-hydratase (LyeJ), and a bisanhydrobacterioruberin hydratase (CruF) (Supplementary Figure S5), which are responsible for the production of bacterioruberin from lycopene. Bacterioruberin is a C_{50} carotenoid pigment known for its antioxidant, anti-inflammatory, immunomodulatory, and antitumoral activities. This pigment is characterized by its red to orange color and complex structure, which includes multiple conjugated double bonds and hydroxyl groups. Additionally, the genome of strain S1BR25-6^T contained a gene encoding lycopene β-cyclase (Supplementary Figure S5), responsible for the production of β-carotene (an orange pigment and vitamin A precursor). The roles of bacterioruberin and β-carotene in photoprotection, antioxidation, and membrane stability are critical for the survival of haloarchaea in harsh environments, while its potential applications in various industries present promising areas for future research (Giani et al., 2020, 2024; Serrano et al., 2022). Strain S1BR25-6^T also harbored the *blh* gene, which encodes β-carotene 15,15'-dioxygenase (Supplementary Figure S5b), responsible for converting β-carotene into retinal. This enzymatic process involves the oxidative cleavage of β-carotene at the 15,15'-double bond, producing two molecules of retinal. Retinal (vitamin A aldehyde) is a key component of microbial rhodopsins, such as bacteriorhodopsin (present in strain S1BR25-6^T and *Halogeometricum rufum* CGMCC 1.7736^T), halorhodopsin (found in *Halogeometricum rufum* CGMCC 1.7736^T), and sensory rhodopsins (identified in *Halogeometricum rufum* CGMCC 1.7736^T and *Halogeometricum limi* CGMCC 1.8711^T). These rhodopsins are involved in phototaxis, energy production through proton pumping, ion transport, and photoprotection (Engelhard et al., 2018). Additionally, retinal has several biotechnological applications. It is used in optogenetics to control cell activity with light and in synthetic biology to create light-sensitive systems (Boyden et al., 2005). It also finds applications in optobioelectronics, gene therapy, and cosmetics for its photoreceptive and antioxidative properties (Maguire et al., 2008; Rouvrais et al., 2018; Paltrinieri et al., 2021).

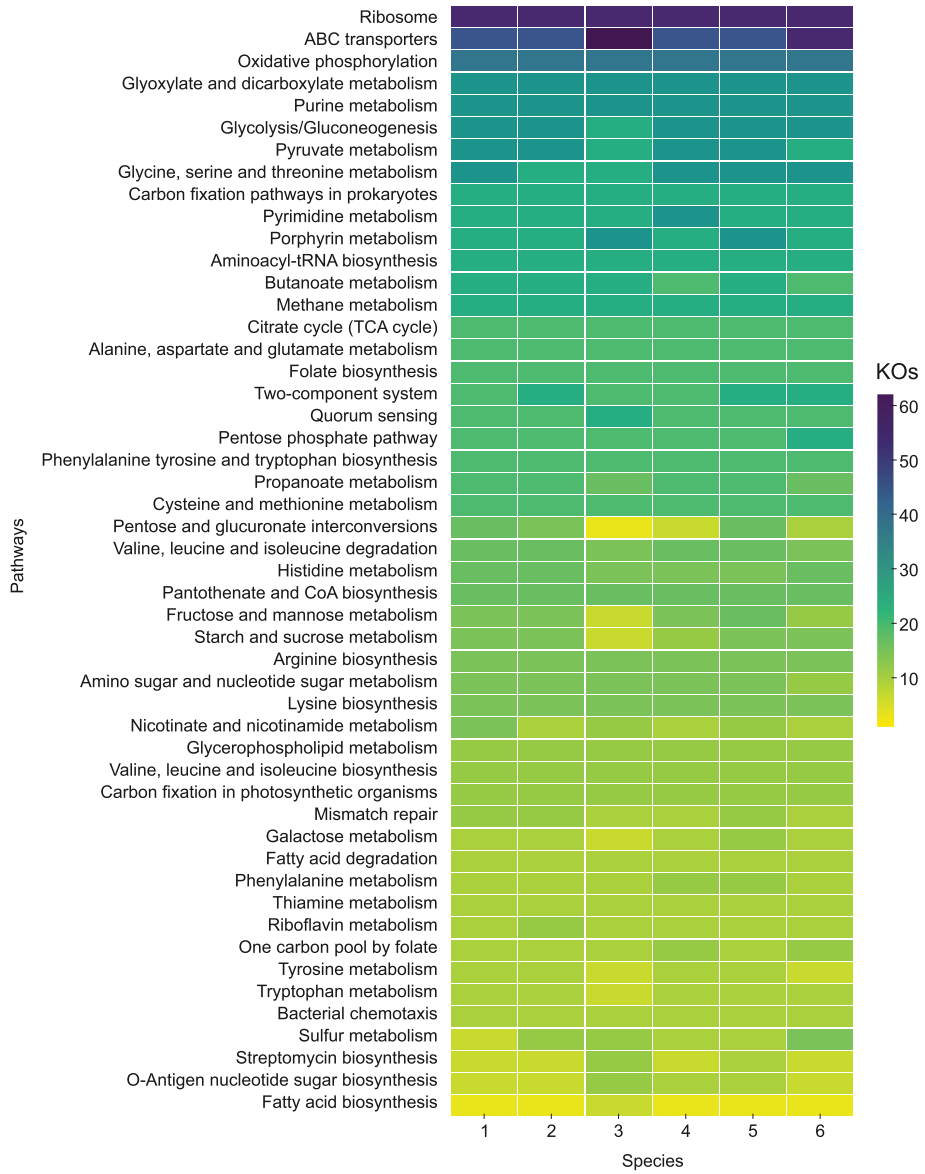

FIGURE 8
Predominant metabolic pathways grouped and ranked by frequency of KO Identifiers (KOs) within KEGG categories. 1. Strain S1BR25-6^{T}; 2. Strain S3BR25-2^{T}; 3. *Halogeometricum borinquense* DSM 11551^{T}; 4. *Halogeometricum limi* CGMCC 1.8711^{T}; 5. *Halogeometricum pallidum* JCM 14848^{T}; 6. *Halogeometricum rufum* CGMCC 1.7736^{T}.

3.7 Thiamine biosynthesis in the genus *Halogeometricum*: bridging bacterial and eukaryotic pathways

The processes involved in thiamine biosynthesis vary among domains *Bacteria*, *Eukarya*, and *Archaea* (Rodionov et al., 2002). In all cases thiamine production involves the separate synthesis of aminopyrimidine and thiazole moieties, which are subsequently coupled to yield thiamine monophosphate (ThMP), that is then phosphorylated to ThDP (Jurgenson et al., 2009). *Archaea* merge strategies from both the bacterial and eukaryotic synthesis pathways (Hayashi et al., 2015). The archaeal thiamine synthesis *de novo* initiates with 5′-phosphoribosyl-5-aminoimidazole (AIR), a byproduct of purine synthesis produced by the enzyme PurM (Figure 9). AIR is then converted to 4-amino-5-hydroxymethyl-2-methylpyrimidine phosphate (HMP-P) by a radical SAM enzyme ThiC, which is also involved in thiamine biosynthesis in *Bacteria* (Lawhorn et al., 2004). ThiD domain protein functions as two-purpose enzyme. In the *de novo* biosynthesis pathway, it catalyzes the phosphorylation of HMP-P to HMP-PP (4-aminohydroxymethyl-2-methylpyrimidine diphosphate), and in the salvage pathway, ThiD sequentially phosphorylates HMP (4-amino-5-hydroxymethyl-2-methylpyrimidine) to HMP-PP (Maupin-Furlow, 2018). To form a thiazole ring, Thi4, a eukaryotic-like protein homolog is used in *Archaea* and distinct strategies for sulfur incorporation are based on the utilization of specific amino acids within its active site. Thi4 with an active-site cysteine residue catalyzes the conversion of NAD (nicotinamide adenine dinucleotide) and glycine to the adenylated

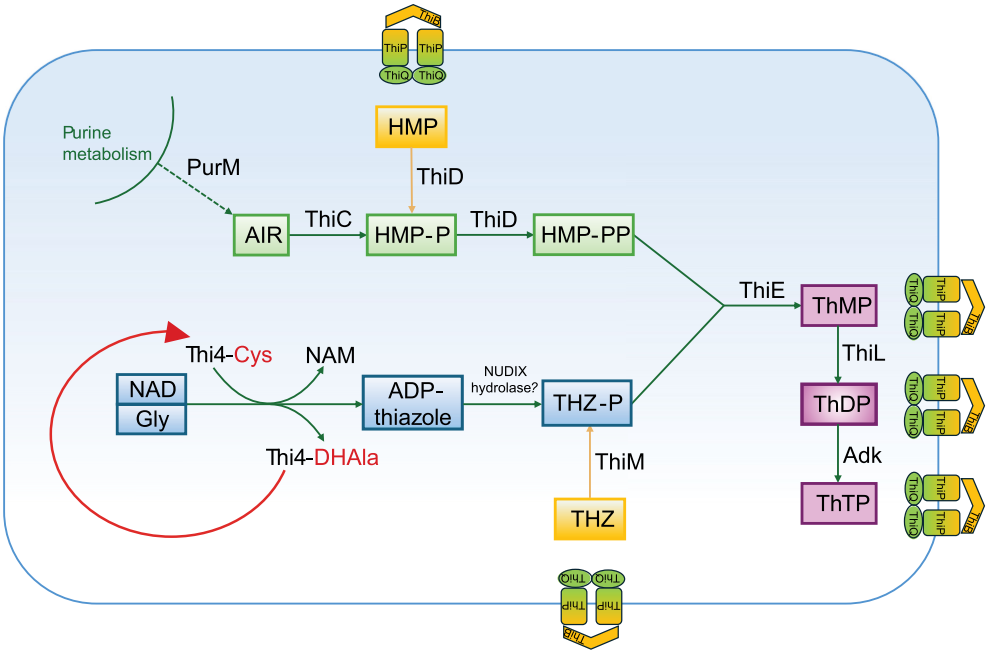

FIGURE 9
A simplified thiamine biosynthetic pathway present in strain S1BR25-6^T, *Halogeometricum borinquense* DSM 11551^T, *Halogeometricum limi* CGMCC 1.8711^T, and *Halogeometricum pallidum* JCM 14848^T based on functional genomic analysis. ADP-thiazole, ADP-5-ethyl-4-methylthiazole-2-carboxylate; AIR, 5′-phosphoribosyl-5-aminoimidazole; Cys, cysteine; DHAla, dehydroalanine; Gly, glycine; HMP, 4-amino-5-hydroxymethyl-2-methylpyrimidine; HMP-P, 4-amino-5-hydroxymethyl-2-methylpyrimidine phosphate; HMP-PP, 4-amino-5-hydroxymethyl-2-methylpyrimidine diphosphate; NAD, nicotinamide adenine dinucleotide; NAM, nicotinamide; ThMP, thiamine monophosphate; ThDP, thiamine diphosphate; ThTP, thiamine triphosphate; THZ, 4-methyl-5-(β-hydroxyethyl) thiazole; THZ-P, 4-methyl-5-(β-hydroxyethyl) thiazole phosphate. The enzymes are discussed in the text.

thiazole (ADP-thiazole) in a single-turnover reaction analogous to that observed in yeasts. Thi4 possessing active-site histidine, found in methanogens and thermococci, catalyzes the synthesis of ADP-thiazole from NAD, glycine, and exogenous sulfide (Eser et al., 2016). The conversion of ADP-thiazole to THZ-P (4-methyl-5-[β-hydroxyethyl] thiazole phosphate) is speculated to be mediated by a NUDIX hydrolase (Sheikh et al., 1998). The condensation of HMP-PP with THZ-P to form ThMP is mediated by two alternative enzymes, ThiE or a recombinant ThiDN (Hayashi et al., 2014). Finally, ThMP is phosphorylated by ThiL to biologically active form, ThDP (Kim et al., 2020) (Figure 9). In haloarchaea, a transcription factor, ThiR has been observed to suppress the expression of genes involved in thiamine biosynthesis (*thi4* and *thiC*) when there is an adequate supply of thiamine (Rodionov et al., 2017; Hwang et al., 2017). Furthermore, in bacteria and eukaryotes, adenylate kinase (Adk) catalyzes the synthesis of thiamine triphosphate (ThTP) from ThDP (Figure 9), suggesting its potential involvement in crucial biological processes such as energy metabolism, adaptation to environmental stress, and possibly cellular signaling (Bettendorff and Wins, 2009; Bettendorff, 2021). The presence and roles of ThTP in archaea remain less elucidated, however archaeal biochemistry often shares similarities with both bacterial and eukaryotic systems, implying that enzymes known to participate in ThTP synthesis in other domains might also be relevant in archaeal species.

Comprehensive metabolic mapping of the species of the genus *Halogeometricum* has revealed that most species within this genus possesses the complete pathway for thiamine biosynthesis, meaning that they have the potential capacity to *de novo* synthesize vitamin B_1. All genes necessary for thiamine biosynthesis in archaea have been detected in *Halogeometricum borinquense* DSM 11551^T, *Halogeometricum limi* CGMCC 1.8711^T, *Halogeometricum pallidum* JCM 14848^T, and the studied strain S1BR25-6^T (Figure 10, Supplementary Figure S5). *Halogeometricum rufum* CGMCC 1.7736^T and strain S3BR25-2^T lack the *thiC* gene which encodes the enzyme required in the first step for the formation of the aminopyrimidine moiety (Figure 9), rendering the thiamine pathway incomplete within the two strains. Only 1% of all prokaryotic genomes in the SEED database (Overbeek et al., 2014) contain a homolog that clusters to the Thi4 family of proteins, among which the majority possess an active-site histidine residue (Sun et al., 2019). The active sites of Thi4 homologs in *Halogeometricum* genomes were identified according to Hwang et al. (2014), and all strains contained a cysteine residue corresponding to the catalytic cysteine residue (Cys165) of *Haloferax volcanii* (HVO_0665) (Figure 10). Based on previous studies (Hwang et al., 2014; Zhang et al., 2016; Sun et al., 2019), it is postulated that Thi4-mediated synthesis of ADP-thiazole involves the use of nicotinamide adenine dinucleotide (NAD), glycine (Gly), and a sulfur atom transferred from an active-site cysteine (Cys) residue. Thi4 functions through a single-turnover mechanism, using a Cys-residue at its active site as a sulfur donor, which becomes inactivated after one reaction cycle, converting into dehydroalanine (DHAla) (Figure 9). The inactive DHAla form of Thi4 is then degraded. Studies focused on exploring alternatives to

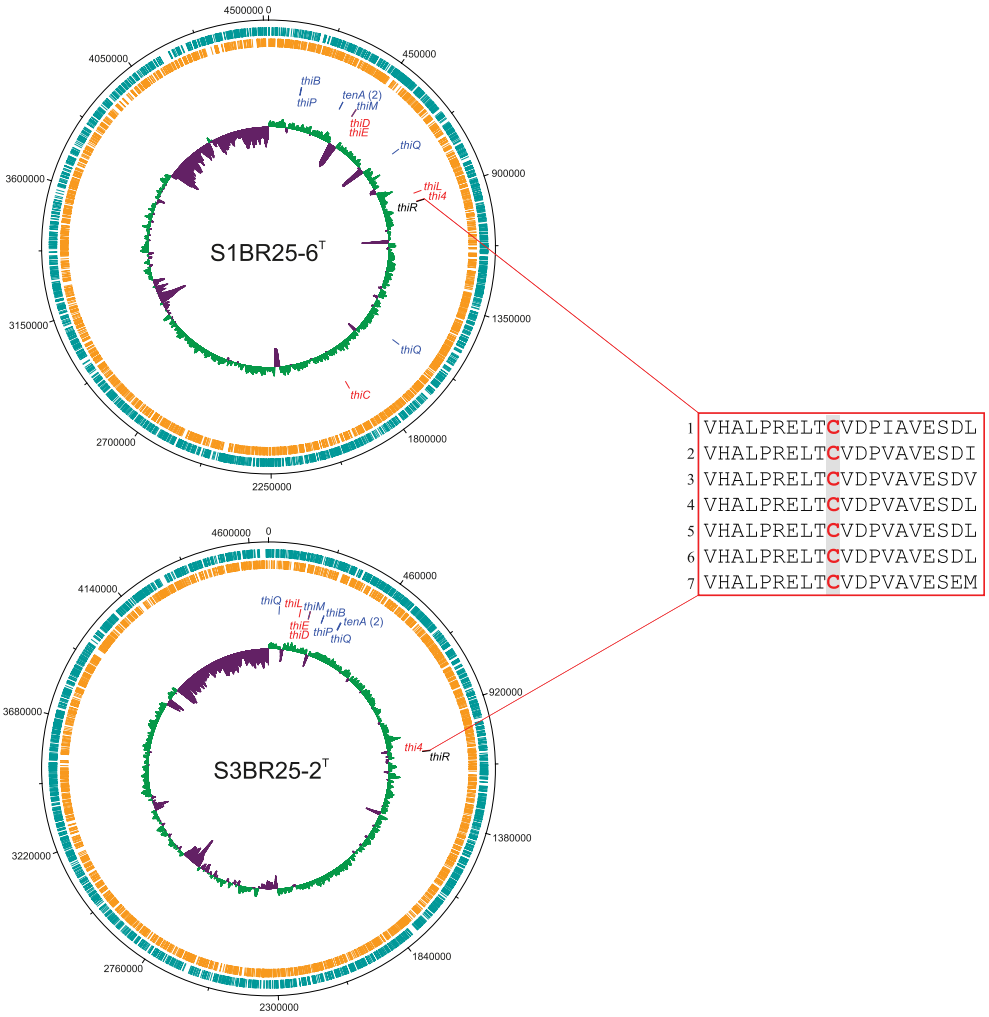

FIGURE 10
Circular representation of the genomes of strains S1BR25-6^T, and S3BR25-2^T. From the outermost to the innermost circles, the genome map displays coding sequences in the leading strand (turquoise); coding sequences in the lagging strand (orange); genes associated with thiamine biosynthesis; and the G+C skew, with violet indicating values below the average and green representing values above the average. Genes involved in the thiamine biosynthesis (and salvage pathway) are displayed in red, genes involved in salvage pathway or thiamine transport system are differentiated by blue color and a gene associated with the thiamine regulation is shown in black. Most of the genes related to thiamine biosynthesis have been clustered within operons allowing for the coordinated regulation of these genes (Yan and Moult, 2006). The red box displays a partial alignment of protein sequences of Thi4 homologs encoded by *thi4* genes. Protein sequences were aligned using ClustalW v.2.1 (Larkin et al., 2007). Residues in analogous position to conserved active-site cysteine (Cys165) of *Haloferax volcanii* (HVO_0665) are highlighted in red. 1. *Haloferax volcanii* (HVO_0665); 2. Strain S1BR25-6^T; 3. Strain S3BR25-2^T; 4. *Halogeometricum borinquense* DSM 11551^T; 5. *Halogeometricum limi* CGMCC 1.8711^T; 6. *Halogeometricum pallidum* JCM 14848^T; 7. *Halogeometricum rufum* CGMCC 1.7736^T.

the suicidal Thi4 pathway to incorporate sulfur into the thiazole moiety of thiamine outlines possible biosynthetic approaches on yeasts (Eser et al., 2016), and plants (Sun et al., 2019). The question of why then certain archaea, yeasts, and plants opt for the single-turnover Thi4 pathway for thiazole biosynthesis instead of utilizing exogenous sulfide remains unanswered. The single-turnover nature of Thi4 might serve as a regulatory mechanism to control the production of thiamine and its precursors. By limiting the reaction to a single event per enzyme molecule, the cell might prevent excessive accumulation of thiamine (Hwang et al., 2014). Furthermore, the thiamine transporter ThiBPQ, predicted in archaea based on homology to bacterial transport systems, facilitates the uptake of thiamine and its phosphorylated derivatives across the cell membrane for direct utilization (Begley et al., 1999) (Figure 9). Additionally, thiamine precursors retrieved from the environment by means of ThiBPQ transport are harnessed in salvage pathways (Hwang et al., 2014; Maupin-Furlow, 2018). It is anticipated that salvage pathway in archaea incorporate enzymes from *de novo* biosynthesis (ThiD, ThiE or ThiDN, and ThiL) alongside enzymes unique to salvage, such as ThiM and TenA (Figure 9). The role of ThiM is phosphorylation of 4-methyl-5-(β-hydroxyethyl) thiazole (THZ), while TenA is involved in salvaging base-degraded forms of thiamine (Jenkins et al., 2007). All *Halogeometricum* species, including the two novel strains, possess genes encoding enzymes for the salvage of thiamine (Supplementary Figure S5).

De novo synthesis of thiamine is a metabolically expensive pathway (Hanson et al., 2018), and auxotrophy can offer an

individual organism the advantage of reducing its metabolic burden. However, microorganisms that produce thiamine to share with their community members gain a crucial position of importance, as they become essential to the consortium's survival (Sathe et al., 2022). The complete pathway for vitamin B_1 biosynthesis is not yet fully understood, and investigating the metabolic processes for *de novo* thiamine production can unveil new opportunities for thiamine-related biotechnological applications, e.g. enhanced microbial production of thiamine, agricultural improvements (Dong et al., 2015), and the development of novel antimicrobial strategies (Kim et al., 2020).

3.8 Adaptations for survival in heavy metals contaminated habitats and archaeal defense mechanisms

As mentioned previously, levels of heavy metals, including copper, lead, cadmium, arsenic, and zinc, were elevated in the studied hypersaline region, contributing to the soil contamination observed in the Odiel Saltmarshes. *Halogeometricum* species, especially the two novel strains S3BR25-2^T and S1BR25-6^T, contained genes involved in heavy metal resistance, emphasizing their evolutionary adaptations to environmental stressors. Each of the analyzed species, except for *Halogeometricum borinquense* DSM 11551^T harbored the *arsC* gene, encoding arsenate reductase, which converts arsenate (As^{5+}) to arsenite (As^{3+}), a form that can be more easily ejected from the cell (Chauhan et al., 2019). The Acr3 antiporter, which expels arsenite from the cells (Lv et al., 2022), was only found in strains S1BR25-6^T and S3BR25-2^T. Its function has been found to be enhanced in the presence of *arsA* (Castillo and Saier, 2010), a gene that was annotated in all *Halogeometricum* members. ArsR, also present in all six strains, is a transcriptional repressor protein involved in the regulation of the *ars* operon. In addition, the *arsM* gene, encoding ArsM, an As(III) S-adenosylmethionine methyl transferase, was present in strains S1BR25-6^T and S3BR25-2^T, as well as *Halogeometricum limi* CGMCC 1.8711^T and *Halogeometricum rufum* CGMCC 1.7736^T. This enzyme is involved in the detoxification and resistance mechanisms against arsenic (Ben Fekih et al., 2018). The *zntA* gene encodes a Zn(II)-translocating P-type ATPase (ZntA), which functions as an efflux pump, using energy from ATP hydrolysis to transport zinc (Zn^{2+}) and other divalent metal cations such as cadmium (Cd^{2+}) and lead (Pb^{2+}) out of the cell (Rensing et al., 1997). This gene was identified in all *Halogeometricum* strains, with strain S3BR25-2^T possessing six copies (Supplementary Figure S5). The *copA* gene, which encodes a P-type ATPase facilitating the active expulsion of copper ions Cu(I) from the cell (Rensing et al., 2000), was identified in all species of the genus *Halogeometricum*. In addition, copper metallochaperones present in strain S1BR25-6^T and *Halogeometricum limi* CGMCC 1.8711^T deliver copper to CopA or other copper-utilizing enzymes and pumps to ensure copper homeostasis (Multhaup et al., 2001). The CzcD transporter present in strains S3BR25-2^T and S1BR25-6^T is a member of the cation diffusion facilitator (CDF) family, which is essential in providing resistance to several heavy metals, including zinc, cadmium, and cobalt (Anton et al., 1999). In addition, *merA* gene, which encodes mercuric reductase, was detected in the genomes of strain S3BR25-2^T and *Halogeometricum pallidum* JCM 14848^T. However, previous studies (Trojańska et al., 2022) suggest that *merA* alone may not be a comprehensive marker of mercury resistance and further research to identify additional genes or mechanisms must be carried out. The exposure to heavy metals frequently results in oxidative stress. The genes encoding superoxide dismutases (sod), catalases (kat), and peroxiredoxins (prx), which are found in all *Halogeometricum* genomes (Supplementary Figure S5), become upregulated in response to heavy metal stress. This upregulation aids in reducing the oxidative damage caused by heavy metals (Ribeiro et al., 2017; Gallego et al., 1996). At trace concentrations (nanomolar to micromolar range), heavy metals, such as cobalt, copper, and zinc act as essential micronutrients, aiding metabolic reactions and enzyme stabilization (Srivastava and Kowshik, 2013; Bruins et al., 2000). Arsenic, on the other hand, can serve as an electron acceptor during anaerobic respiration in archaea and bacteria (Dowdle et al., 1996). However, at higher concentrations (above 1 mM), heavy metals become harmful cellular toxins to various ecosystem components, including the human body (Tchounwou et al., 2012; Voica et al., 2016). Environmental increases in heavy metal concentrations often trigger the activation of resistance mechanisms (Srivastava and Kowshik, 2013). The determination of the MIC for five heavy metals was performed for the two novel strains to validate the previous genomic analysis. The tolerance levels of the isolated strains to the tested heavy metals followed the order $Cu^{2+} < Zn^{2+} < Pb^{2+} < Cd^{2+} < As^{5+}$. The MICs for these heavy metals in the two halobacterial strains are summarized in Table 1. Experimental results confirmed that strains S1BR25-6^T and S3BR25-2^T could tolerate arsenate concentrations up to 700 mM. The highest tolerance of haloarchaea to arsenate (As^{5+}) reported to date is 250 mM, as observed in several *Halorubrum* species (Ordoñez et al., 2018). In contrast, multiple studies indicated the cadmium tolerance in haloarchaea up to 4 mM (Nieto et al., 1987; Das et al., 2014; Braganca and Furtado, 2017; Baati et al., 2020; Vera-Bernal and Martínez-Espinosa, 2021). In a recent investigation by Tavoosi et al. (2023), four haloarchaeal strains demonstrated the ability to grow in the presence of 16 mM Cd^{2+}. Strains S1BR25-6^T and S3BR25-2^T exhibited even greater cadmium tolerance, withstanding concentrations up to 50 mM. Both novel strains were able to grow in the presence of 5 mM lead. The results showed that strain S1BR25-6^T had a relatively high susceptibility to zinc, with a MIC of 0.5 mM. It was demonstrated that high concentrations of NaCl increase the toxicity of zinc due to the formation of more soluble zinc chloride species (such as $ZnCl_2$), which enhances the bioavailability of zinc for microorganisms (Nieto et al., 1987; Baati et al., 2020). Tavoosi et al. (2023) reported the highest tolerance to zinc among haloarchaeal strains up to date, with eight strains demonstrating exceptional tolerance levels, capable of withstanding zinc concentrations up to 4 mM. Similarly, strain S3BR25-2^T in the current study exhibited comparable zinc tolerance, enduring concentrations up to 4 mM. The highest toxicities were observed with copper, as indicated by their lower MIC values, which did not exceed 2.5 mM.

TABLE 1 Tolerance levels of the two novel strains, S1BR25-6^T and S3BR25-2^T to various concentrations (mM) of heavy metals.

Heavy metal	Concentration (mM)	S1BR25-6^T	S3BR25-2^T
As^{5+}	0.01	+	+
	0.5	+	+
	1	+	+
	2.5	+	+
	4	+	+
	5	+	+
	10	+	+
	20	+	+
	50	+	+
	80	+	+
	100	+	+
	150	+	+
	200	+	+
	300	+	+
	500	+	+
	600	+	+
	700	+	+
Cd^{2+}	0.01	+	+
	0.5	+	+
	1	+	+
	2.5	+	+
	4	+	+
	5	+	+
	10	+	+
	20	+	+
	50	+	+
	80	–	–
Cu^{2+}	0.01	+	+
	0.5	+	+
	1	+	+
	2.5	–	–
Pb^{2+}	0.01	+	+
	0.5	+	+
	1	+	+
	2.5	+	+
	4	+	+
	5	+	+
	10	–	–
Zn^{2+}	0.01	+	+
	0.05	+	+
	0.5	–	+
	1	–	+
	2.5	–	+
	4	–	+
	5	–	–

(Continued)

TABLE 1 Continued

+, growth; -, absence of growth.

In summary, given the high levels of heavy metals, particularly arsenic and zinc, as well as elevated concentrations of cadmium, lead, and copper in the hypersaline soils of the Odiel Saltmarshes (Huelva), it was anticipated that the strains isolated from these environments would exhibit tolerance and/or resistance to these heavy metals. The *in silico* functional genomic analysis identified genes associated with heavy metal resistance in *Halogeometricum* species, including the two novel strains. Experimental study of strains S1BR25-6^T and S3BR25-2^T corroborated their tolerance to heavy metals, indicating their potential for bioremediation applications in contaminated hypersaline environments.

Furthermore, prokaryotes possessing a CRISPR-Cas immune system contain arrays of repeated sequences interspersed with short segments (spacers) derived from foreign genetic elements near the *cas* gene clusters (Mojica et al., 2005). Strain S3BR25-2^T harbored genes associated with the CRISPR-Cas system, displaying a type IB *cas* gene cluster incorporating 51 spacers. Other *Halogeometricum* species deploy alternative defense strategies, such as the Restriction-Modification (R-M) and the Toxin-Antitoxin (TA) systems (Supplementary Figure S5).

3.9 The dual strategies for osmoregulation in *Halogeometricum* species

The members of the class *Halobacteria* excel in the process of osmoadaptation, allowing them to thrive in extremely hypersaline habitats. They are well adapted to endure significant salinity fluctuations that result from rainfall and evaporation. Haloarchaea are often categorized as adopting a "salt-in" strategy, accumulating inorganic ions, mainly K^+ and Cl^-, directly from their environment to combat osmotic stress (Müller et al., 2005), while Na^+ ions are extruded from cells. Conversely, the "salt-out" strategy involves the accumulation of organic molecules to counteract external osmotic pressure without increasing internal ionic strength to detrimental levels (Gunde-Cimerman et al., 2018). Species within the genus *Halogeometricum* exhibit diverse ion transport mechanisms to effectively adapt to changing salinity levels (Supplementary Figure S5). During hyper-osmotic shock, the processes of importing potassium and expelling sodium are facilitated through a proton gradient that is generated either by the direct activation of proton

translocation through bacteriorhodopsin under light exposure or via respiratory electron transport mechanisms (Becker et al., 2014). Specific transporters responsible for expelling Na^+, absorbing K^+, and regulating Cl^- balance were observed in the species of the genus *Halogeometricum*. All studied species possessed the capability to eject sodium through the mechanism of YrbG Na^+/Ca^{2+} antiport systems, and to allow the efflux of small osmolytes and water upon activation of MscS mechanosensitive channel during hypo-osmotic shock (Anishkin et al., 2008). Studies have demonstrated that the organic solutes trehalose and glycine betaine are ubiquitously found in extremely halophilic archaea, acquired either through *de novo* synthesis or by environmental uptake (Youssef et al., 2014). Genomic analysis revealed the presence of genes involved in biosynthesis of trehalose by OtsAB pathway in all *Halogeometricum* members except of *Halogeometricum borinquense* DSM 11551^T. However, all six species possessed genes that encode a transport protein facilitating the uptake of a range of compatible solutes, such as choline, glycine betaine, proline betaine, ectoine as well as trehalose. In addition, strains S1BR25-6^T and S3BR25-2^T, and the phylogenetically closest *Halogeometricum pallidum* JCM 14848^T exhibited ABC transporters of the Opu family that function in the uptake of compatible solutes, particularly glycine betaine and related osmoprotectants (Kappes et al., 1999). Based on the genome analysis, the genus *Halogeometricum* can exhibit flexibility in the osmoregulation, potentially employing both, "salt-in" and "salt-out" strategies depending on the severity of the osmotic stress and the availability of resources. This adaptability has been similarly observed in species of the genus *Halomicroarcula* (now reclassified as *Haloarcula*) (Durán-Viseras et al., 2021) and, more recently, in *Halorubrum kocurii* 2020YC7, which switch between the accumulation of potassium ions and compatible solutes such as trehalose and glycine betaine (Ding et al., 2022).

Besides their ability to quickly adapt to shifts in environmental salinity, adaptations of haloarchaea to high-salt conditions further include the acidification of their proteome and an increased genomic G+C content (Becker et al., 2014). We have performed a proteomic analysis of all *Halogeometricum* genomes together with others from representative species of the family *Haloferacaceae*. To examine the differences in protein acidity, the proteomes of the *Halogeometricum* species were compared to those from "salt-in" halophilic prokaryotes such as *Haloquadratum walsbyi* C23^T, *Halorubrum saccharovorum* DSM 1137^T, and *Salinibacter ruber* DSM 13855^T, as well as to the proteome of a "salt-out" bacterium, *Spiribacter salinus* M19-40^T. Strains S1BR25-6^T and S3BR25-2^T along with species within the genus *Halogeometricum* and other type species of the family *Haloferacaceae* exhibited both, high genomic G+C content (ranging 59.9–68.0 mol%) and a significantly acidic proteome. This is demonstrated by an isoelectric point profile with a major peak at around 4 (Supplementary Figure S6), indicating a preference for a "salt-in" osmoregulation strategy (Becker et al., 2014). However, a minor peak at around 10 indicated the presence of a significant number of basic proteins, which may include certain types of enzymes, transcription factors, and membrane proteins that require a positive charge for their function or interaction with other cellular components, such as DNA or negatively charged cell membranes (Becker et al., 2014). In summary, the bimodal distribution of isoelectric points reflects a balance between the general adaptation of halophilic organisms to high-salt environments through the acidification of their proteome and the necessity for basic proteins that fulfill specific cellular roles.

4 Conclusions

Traditional techniques based on the culture-based methods enabled us to isolate in pure culture and to characterize initially the strains isolated from hypersaline soils located in Odiel Saltmarshes, a natural area of tidal wetlands located at the estuary of the Odiel and Tinto rivers, with the confluence of the Atlantic Ocean, in Southwestern Spain. This study undertakes a detailed genomic comparison within the genus *Halogeometricum*, identifying key aspects such as metabolic capabilities, osmoregulatory strategies, and heavy metal resistance. The discovery of a dual osmoregulatory mechanism through *in-silico* analysis, which merges "salt-in" and "salt-out" strategies, underlines the adaptive versatility of these species. Additionally, the capacity for *de novo* thiamine production in strain S1BR25-6^T and related *Halogeometricum* species emphasizes their metabolic complexity, suggesting their significant roles in ecosystem functionality and their potential in biotechnological applications. Experimental analysis of strains S1BR25-6^T and S3BR25-2^T confirmed their tolerance to heavy metals, particularly arsenic, cadmium, and lead, emphasizing their potential for bioremediation applications. Metagenomic fragment recruitment analysis across various datasets has particularly highlighted the dominance of *Halogeometricum* species in the Odiel Saltmarshes hypersaline soils and in the brines of saltern ponds with high salinity, reinforcing our knowledge of their extremely halophilic nature. Further taxonomic characterization of the studied strains, S1BR25-6^T and S3BR25-2^T, included phenotypic and chemotaxonomic analysis, as well as genome-based techniques. This study shows that strains S1BR25-6^T and S3BR25-2^T represent two novel species of the genus *Halogeometricum*, for which we propose the names *Halogeometricum salsisoli* sp. nov. and *Halogeometricum luteum* sp. nov., respectively. The detailed descriptions of the two new species are stated below.

Description of *Halogeometricum salsisoli* sp. nov.

Halogeometricum salsisoli (sal.si.so'li. L. perf. part. *salsus*, salty; L. neut. adj. *solum*, soil; N.L. gen. n. *salsisoli*, of salty soil).

Cells are Gram-stain-negative, non-motile, irregular cocci with 1.5–2 µm. Colonies are pink pigmented, elevated, round, and mucoid on R2A 25 agar medium after 7 days of incubation at 37°C. No growth occurs anaerobically with dimethyl sulfoxide (DMSO), L-arginine, or potassium nitrate. Extremely halophilic, able to grow in media with 10–30% (w/v) NaCl, with optimal growth at 25% (w/v) NaCl. Optimal growth occurs at pH and temperature of 7.0 and 37°C, respectively. The pH and temperature ranges permitting growth are 6.0–8.5 and 20–50°C, respectively. Catalase-positive, oxidase-negative. Aesculin is strongly hydrolyzed but casein, gelatin, starch, and Tween 80 are not. Nitrate and nitrite are reduced. H_2S and indole are not produced. Methyl red test is positive whereas Voges-Proskauer and Simmons' citrate tests are negative. Acid is produced from D-arabinose, D-fructose, D-galactose,

D-glucose, D-trehalose, D-xylose, glycerol, lactose, maltose, and sucrose and is not produced from mannitol. The following compounds are used as sole carbon and energy sources: acetate, benzoate, butyrate, D-arabinose, D-cellobiose, D-fructose, D-glucose, D-ribose, D-xylose, formate, fumarate, lactose, mannose, melezitose, melibiose, pyruvate, salicin, and sucrose, whereas citrate, D-sorbitol, dulcitol, hippurate, L-glutamate, mannitol, propionate, and xylitol are not. L-glycine, L-glutamine, L-serine, and L-threonine are used as sole carbon, nitrogen, and energy sources and L-alanine, L-arginine are not. The major polar lipids are phosphatidylglycerol (PG), phosphatidylglycerol phosphate methyl ester (PGP-Me), and a glycolipid chromatographically identical to sulfated diglycosyl diether (S-DGD-1). Traces of biphosphatidylglycerol (BPG) and minor unidentified glycolipids are present. Phosphatidylglycerol sulfate (PGS) is absent. The DNA G+C content is 65.5 mol%.

The type strain is S1BR25-6^T (= CCM 9250^T = CECT 30624^T), isolated from a hypersaline soil from the Odiel Saltmarshes Natural Area, located at the estuary of the Odiel and Tinto rivers, with the confluence of the Atlantic Ocean, in Huelva, Spain

The GenBank/EMBL/DDBJ accession numbers for the 16S rRNA and *rpoB'* gene sequences of strain S1BR25-6^T are ON653036 and ON668042, respectively. The GenBank/EMBL/DDBJ accession number of the whole genome sequence of strain S1BR25-6^T is JAMQOP000000000.

Description of *Halogeometricum luteum* sp. nov.

Halogeometricum luteum (lu.te'um. L. neut. adj. *luteum*, orange colored).

Cells are Gram-stain-negative, motile, and pleomorphic (rods and irregular cocci) with 0.5–1.5 × 1–3 µm. Colonies have a pale orange pigmentation, they are elevated, round, and mucoid on R2A 25 agar medium after 7 days of incubation at 37°C. No growth occurs anaerobically with dimethyl sulfoxide (DMSO), L-arginine, or potassium nitrate. Extremely halophilic, able to grow in media with 12–30% (w/v) NaCl, with optimal growth at 25% (w/v) NaCl. Optimal growth occurs at pH and temperature of 7.0 and 37°C, respectively. The pH and temperature ranges permitting growth are 6.0–8.5 and 20–50°C, respectively. Catalase-positive, oxidase-negative. Aesculin is hydrolyzed but casein, gelatin, starch, and Tween 80 are not. Nitrate and nitrite are reduced. H_2S and indole are not produced. Methyl red test is positive whereas Voges-Proskauer and Simmons' citrate tests are negative. Acid is produced from D-arabinose, D-fructose, D-galactose, D-glucose, D-trehalose, D-xylose, glycerol, maltose, mannitol, and sucrose but is not produced from lactose. The following compounds are used as sole carbon and energy sources: D-fructose, D-glucose, D-ribose, D-xylose, dulcitol, hippurate, mannitol, mannose, melezitose, pyruvate, salicin, and sucrose, whereas acetate, benzoate, citrate, butyrate, D-arabinose, D-cellobiose, D-sorbitol, formate, fumarate, lactose, L-glutamate, melibiose, propionate, and xylitol are not. L-alanine, L-arginine, L-glycine, and L-glutamine are used as sole carbon, nitrogen, and energy sources but L-serine, and L-threonine are not. The major polar lipids are phosphatidylglycerol (PG), phosphatidylglycerol phosphate methyl ester (PGP-Me), and a glycolipid chromatographically identical to sulfated diglycosyl diether (S-DGD-1). Traces of biphosphatidylglycerol (BPG) and minor unidentified glycolipids are present. Phosphatidylglycerol sulfate (PGS) is absent. The DNA G+C content is 66.0 mol%.

The type strain is S3BR25-2^T (= CCM 9253^T = CECT 30622^T), isolated from a hypersaline soil from the Odiel Saltmarshes Natural Area, located at the estuary of the Odiel and Tinto rivers, with the confluence of the Atlantic Ocean, in Huelva, Spain.

The GenBank/EMBL/DDBJ accession numbers for the 16S rRNA and *rpoB'* gene sequences of strain S3BR25-2^T are ON682483 and ON668043, respectively. The GenBank/EMBL/DDBJ accession number of the whole genome sequence of strain S3BR25-2^T is JAMQOQ000000000.

Data availability statement

The datasets presented in this study can be found in online repositories. The names of the repositories and accession numbers can be found below: https://www.ncbi.nlm.nih.gov/genbank/, the 16S rRNA and *rpoB'* genes and the genome sequences generated for this study can be found in the GenBank/EMBL/DDBJ database under the accession numbers ON653036, ON682483, ON668042, ON668043, JAMQOP000000000 and JAMQOQ000000000, for *Halogeometricum salsisoli* S1BR25-6^T and *Halogeometricum luteum* S3BR25-2^T, respectively.

Author contributions

DS: Formal analysis, Investigation, Writing – original draft, Writing – review & editing. CS-P: Conceptualization, Investigation, Writing – review & editing. RH: Conceptualization, Investigation, Supervision, Writing – review & editing. AV: Conceptualization, Supervision, Writing – review & editing.

Funding

The author(s) declare financial support was received for the research, authorship, and/or publication of this article. This study was supported by grant PID2020-118136GB-I00 funded by MICIU/AEI/10.13039/501100011033 (to AV and CS-P).

Acknowledgments

We thank Aharon Oren for the advice with the nomenclature of the two new species names.

Conflict of interest

The authors declare that the research was conducted in the absence of any commercial or financial relationships that could be construed as a potential conflict of interest.

The author(s) declared that they were an editorial board member of Frontiers, at the time of submission. This had no impact on the peer review process and the final decision.

Publisher's note

All claims expressed in this article are solely those of the authors and do not necessarily represent those of their affiliated organizations, or those of the publisher, the editors and the reviewers. Any product that may be evaluated in this article, or claim that may be made by its manufacturer, is not guaranteed or endorsed by the publisher.

Supplementary material

The Supplementary Material for this article can be found online at: https://www.frontiersin.org/articles/10.3389/fmars.2024.1421769/full#supplementary-material

References

Altschul, S. F., Gish, W., Miller, W., Myers, E. W., and Lipman, D. J. (1990). Basic local alignment search tool. *J. Mol. Biol.* 215, 403–410. doi: 10.1016/S0022-2836(05)80360-2

Alzohairy, A. M. (2011). BioEdit: An important software for molecular biology. *GERF Bull. Biosci.* 2, 60–61.

Angelini, R., Corral, P., Lopalco, P., Ventosa, A., and Corcelli, A. (2012). Novel ether lipid cardiolipins in archaeal membranes of extreme haloalkaliphiles. *Biochim. Biophys. Acta* 1818, 1365–1373. doi: 10.1016/j.bbamem.2012.02.014

Anishkin, A., Kamaraju, K., and Sukharev, S. (2008). Mechanosensitive channel MscS in the open state: modeling of the transition, explicit simulations, and experimental measurements of conductance. *J. Gen. Physiol.* 132, 67–83. doi: 10.1085/jgp.200810000

Anton, A., Große, C., Reißmann, J., Pribyl, T., and Nies, D. H. (1999). CzcD is a heavy metal ion transporter involved in regulation of heavy metal resistance in *Ralstonia* sp. strain CH34. *J. Bacteriol.* 181, 6876–6881. doi: 10.1128/jb.181.22.6876-6881.1999

Arahal, D. R., Dewhirst, F. E., Paster, B. J., Volcani, B. E., and Ventosa, A. (1996). Phylogenetic analyses of some extremely halophilic archaea isolated from dead sea water, determined on the basis of their 16S rRNA sequences. *Appl. Environ. Microbiol.* 62, 3779–3786. doi: 10.1128/aem.62.10.3779-3786.1996

Auch, A. F., von Jan, M., Klenk, H.-P., and Göker, M. (2010). Digital DNA-DNA hybridization for microbial species delineation by means of genome-to-genome sequence comparison. *Stand. Genomic Sci.* 2, 117–134. doi: 10.4056/sigs.531120

Baati, H., Siala, M., Azri, C., Ammar, E., Dunlap, C., and Trigui, M. (2020). Resistance of a *Halobacterium salinarum* isolate from a solar saltern to cadmium, lead, nickel, zinc, and copper. *Antonie van Leeuwenhoek* 113, 1699–1711. doi: 10.1007/s10482-020-01475-6

Becker, E. A., Seitzer, P. M., Tritt, A., Larsen, D., Krusor, M., Yao, A. I., et al. (2014). Phylogenetically driven sequencing of extremely halophilic archaea reveals strategies for static and dynamic osmo-response. *PLoS. Genet.* 1, e1004784. doi: 10.1371/journal.pgen.1004784

Begley, T. P., Downs, D. M., Ealick, S. E., McLafferty, F. W., Van Loon, A. P., Taylor, S., et al. (1999). Thiamin biosynthesis in prokaryotes. *Arch. Microbiol.* 171, 293–300. doi: 10.1007/s002030050713

Ben Fekih, I., Zhang, C., Li, Y. P., Zhao, Y., Alwathnani, H. A., Saquib, Q., et al. (2018). Distribution of arsenic resistance genes in prokaryotes. *Front. Microbiol.* 9. doi: 10.3389/fmicb.2018.02473

Bertola, M., Ferrarini, A., and Visioli, G. (2021). Improvement of soil microbial diversity through sustainable agricultural practices and its evaluation by -omics approaches: A perspective for the environment, food quality and human safety. *Microorganisms* 9, 1400. doi: 10.3390/microorganisms9071400

Bettendorff, L. (2021). Update on thiamine triphosphorylated derivatives and metabolizing enzymatic complexes. *Biomolecules* 11, 1645. doi: 10.3390/biom11111645

Bettendorff, L., and Wins, P. (2009). Thiamine diphosphate in biological chemistry: New aspects of thiamine metabolism, especially triphosphate derivatives acting other than as cofactors. *FEBS J.* 276, 2917–2925. doi: 10.1111/j.1742-4658.2009.07019.x

Boyden, E. S., Zhang, F., Bamberg, E., Nagel, G., and Deisseroth, K. (2005). Millisecond-timescale, genetically targeted optical control of neural activity. *Nat. Neurosci.* 8, 1263–1268. doi: 10.1038/nn1525

Braganca, J., and Furtado, I. (2017). Removal of cadmium by *Halobacterium* strain R1 MTCC 3265 from saline and non-saline econiches. *Indian J. Sci.* 46, 2215–2219.

Bruins, M. R., Kapil, S., and Oehme, F. W. (2000). Microbial resistance to metals in the environment. *Ecotox Environ. Safe* 45, 198–207. doi: 10.1006/eesa.1999.1860

Carver, T., Thomson, N., Bleasby, A., Berriman, M., and Parkhill, J. (2009). DNAPlotter: circular and linear interactive genome visualization. *Bioinformatics* 25, 119–120. doi: 10.1093/bioinformatics/btn578

Castillo, R., and Saier, M. H. (2010). Functional promiscuity of homologues of the bacterial ArsA ATPases. *Int. J. Microbiol.* 187373. doi: 10.1155/2010/187373

Chauhan, D., Srivastava, P. A., Agnihotri, V., Yennamalli, R. M., and Priyadarshini, R. (2019). Structure and function prediction of arsenate reductase from *Deinococcus indicus* DR1. *J. Mol. Model.* 25, 15. doi: 10.1007/s00894-018-3885-3

Chun, J., Oren, A., Ventosa, A., Christensen, H., Arahal, D. R., da Costa, M. S., et al. (2018). Proposed minimal standards for the use of genome data for the taxonomy of prokaryotes. *Int. J. Syst. Evol. Microbiol.* 68, 461–466. doi: 10.1099/ijsem.0.002516

Chun, J., and Rainey, F. A. (2014). Integrating genomics into the taxonomy and systematics of the *Bacteria* and *Archaea*. *Int. J. Syst. Evol. Microbiol.* 64, 316–324. doi: 10.1099/ijs.0.054171-0

Consejería de Medio Ambiente (1999). *Los criterios y estándares para declarar un suelo contaminado en Andalucía y la metodología y técnicas de toma de muestra y análisis para su investigación.* (Sevilla: Junta de Andalucía).

Corral, P., Gutiérrez, M. C., Castillo, A. M., Domínguez, M., Lopalco, P., Corcelli, A., et al. (2013). *Natronococcus roseus* sp. nov., a haloalkaliphilic archaeon from a hypersaline lake. *Int. J. Syst. Evol. Microbiol.* 63, 104–108. doi: 10.1099/ijs.0.036558-0

Couvin, D., Bernheim, A., Toffano-Nioche, C., Touchon, M., Michalik, J., Néron, B., et al. (2018). CRISPRCasFinder, an update of CRISRFinder, includes a portable version, enhanced performance and integrates search for Cas proteins. *Nucleic Acids Res.* 46, W246–W251. doi: 10.1093/nar/gky425

Cowan, S. T., and Steel, K. J. (1993). *Manual for the identification of medical bacteria. 3rd* (Cambridge: Cambridge University Press).

Cui, H.-L., Gao, X., Li, X.-Y., Xu, X.-W., Zhou, Y.-G., Liu, H.-C., et al. (2010a). *Halosarcina limi* sp. nov., a halophilic archaeon from a marine solar saltern, and emended description of the genus *Halosarcina*. *Int. J. Syst. Evol. Microbiol.* 60, 2462–3466. doi: 10.1099/ijs.0.018697-0

Cui, H.-L., Hou, J., Amoozegar, M. A., Dyall-Smith, M. L., de la Haba, R. R., Minegishi, H., et al. (2024). Proposed minimal standards for description of new taxa of the class *Halobacteria*. *Int. J. Syst. Evol. Microbiol.* 74, 6290. doi: 10.1099/ijsem.0.006290

Cui, H.-L., Yang, X., Gao, X., Li, X.-Y., Xu, X.-W., Zhou, Y.-G., et al. (2010b). *Halogeometricum rufum* sp. nov., a halophilic archaeon from a marine solar saltern, and emended description of the genus *Halogeometricum*. *Int. J. Sys.t Evol. Microbiol.* 60, 2613–2617. doi: 10.1099/ijs.0.019463-0

Das, D., Salgaonkar, B. B., Mani, K., and Braganca, J. M. (2014). Cadmium resistance in extremely halophilic archaeon *Haloferax* strain BBK2. *Chemosphere* 112, 385–392. doi: 10.1016/j.chemosphere.2014.04.058

DeLong, E. F. (1992). Archaea in coastal marine environments. *Proc. Natl. Acad. Sci. U.S.A.* 89, 5685–5689. doi: 10.1073/PNAS.89.12.5685

Dhir, S., Tarasenko, M., Napoli, E., and Giulivi, C. (2019). Neurological, psychiatric, and biochemical aspects of thiamine deficiency in children and adults. *Front. Psychiatry* 10. doi: 10.3389/fpsyt.2019.00207

Ding, R., Yang, N., and Liu, J. (2022). The osmoprotectant switch of potassium to compatible solutes in an extremely halophilic archaea *Halorubrum kocurii* 2020YC7. *Genes* 13, 939. doi: 10.3390/genes13060939

Dong, W., Stockwell, V. O., and Goyer, A. (2015). Enhancement of Thiamin content in *Arabidopsis thaliana* by metabolic engineering. *Plant Cell Physiol.* 56, 2285–2296. doi: 10.1093/pcp/pcv148

Dowdle, P. R., Laverman, A. M., and Oremland, R. S. (1996). Bacterial dissimilatory reduction of arsenic (V) to arsenic (III) in anoxic sediments. *Appl. Environ. Microb.* 62, 1664–1669. doi: 10.1128/aem.62.5.1664-1669.1996

Durán-Viseras, A., Sánchez-Porro, C., and Ventosa, A. (2021). Genomic insights into new species of the genus *Halomicroarcula* reveals potential for new osmoadaptative strategies in halophilic archaea. *Front. Microbiol.* 12. doi: 10.3389/fmicb.2021.751746

Dussault, H. P. (1955). An improved technique for staining red halophilic bacteria. *J. Bacteriol.* 70, 484–485. doi: 10.1128/jb.70.4.484-485.1955

Edgar, R. C. (2022). Muscle5: High-accuracy alignment ensembles enable unbiased assessments of sequence homology and phylogeny. *Nat. Commun.* 13, 6968. doi: 10.1038/s41467-022-34630-w

Engelhard, C., Chizhov, I., Siebert, F., and Engelhard, M. (2018). Microbial halorhodopsins: light-driven chloride pumps. *Chem. Rev.* 118, 10629–10645. doi: 10.1021/acs.chemrev.7b00715

Eren, A. M., Esen, Ouml;.C., Quince, C., Vineis, J. H., Morrison, H. G., Sogin, M. L., et al. (2015). Anvi'o: an advanced analysis and visualization platform for 'omics data. *PeerJ.* 3, e1319. doi: 10.7717/peerj.1319

Eser, B. E., Zhang, X., Chanani, P. K., Begley, T. P., and ealick, S. E. (2016). From suicide enzyme to catalyst: the iron-dependent sulfide transfer in *Methanococcus jannaschii* thiamin thiazole biosynthesis. *J. Am. Chem. Soc.* 138, 3639–3642. doi: 10.1021/jacs.6b00445

Felsenstein, J. (1981). Evolutionary trees from DNA sequences: a maximum likelihood approach. *J. Mol. Evol.* 17, 368–376. doi: 10.1007/BF01734359

Felsenstein, J. (1983). Parsimony in systematics: biological and statistical issues. *Annu. Rev. Ecol. Syst.* 14, 313–333. doi: 10.1146/annurev.es.14.110183.001525

Fernández, A. B., Ghai, R., Martin-Cuadrado, A.-B., Sánchez-Porro, C., Rodriguez-Valera, F., and Ventosa, A. (2014). Prokaryotic taxonomic and metabolic diversity of an intermediate salinity hypersaline habitat assessed by metagenomics. *FEMS Microbiol. Ecol.* 88, 623–635. doi: 10.1111/1574-6941.12329

Fullmer, M. S., Soucy, S. M., Swithers, K. S., Makkay, A. M., Wheeler, R., Ventosa, A., et al. (2014). Population and genomic analysis of the genus *Halorubrum*. *Front. Microbiol.* 5. doi: 10.3389/fmicb.2014.00140

Galisteo, C. (2022). *Gitana: phyloGenetic Imaging Tool for Adjusting Nodes and other Arrangements*. Available online at: https://github.com/cristinagalisteo/gitana (Accessed 3 June 2022).

Gallego, S. M., Benavides, M. P., and Tomaro, M. L. (1996). Effect of heavy metal ion excess on sunflower leaves: evidence for involvement of oxidative stress. *Plant Sci.* 121, 151–159. doi: 10.1016/S0168-9452(96)04528-1

Ghai, R., Pašić, L., Fernández, A. B., Martin-Cuadrado, A.-B., Mizuno, C. M., McMahon, K. D., et al. (2011). New abundant microbial groups in aquatic hypersaline environments. *Sci. Rep.* 1, 135. doi: 10.1038/srep00135

Giani, M., Miralles-Robledillo, J., Peiró, G., Pire, C., and Martínez-Espinosa, R. (2020). Deciphering pathways for carotenogenesis in haloarchaea. *Molecules* 25, 1197. doi: 10.3390/molecules25051197

Giani, M., Pire, C., and Martínez-Espinosa, R. M. (2024). Bacterioruberin: biosynthesis, antioxidant activity, and therapeutic applications in cancer and immune pathologies. *Mar. Drugs* 22, 167. doi: 10.3390/md2204016

Goris, J., Konstantinidis, K. T., Klappenbach, J. A., Coenye, T., Vandamme, P., and Tiedje, J. M. (2007). DNA-DNA hybridization values and their relationship to whole-genome sequence similarities. *Int. J. Syst. Evol. Microbiol.* 57, 81–91. doi: 10.1099/ijs.0.64483-0

Grande, J., Borrego, J., de la Torre, M. L., and Sáinz, A. (2003). Application of cluster analysis to the geochemistry zonation of the estuary waters in the tinto and odiel rivers (Huelva, Spain). *Environ. Geochem. Health* 25, 233–246. doi: 10.1023/A:1023217318890

Gunde-Cimerman, N., Plemenitaš, A., and Oren, A. (2018). Strategies of adaptation of microorganisms of the three domains of life to high salt concentrations. *FEMS Microbiol. Rev.* 42, 353–375. doi: 10.1093/femsre/fuy009

Hall, B. G. (1982). Evolution of a regulated operon in the laboratory. *Genetics* 101, 335–344. doi: 10.1093/genetics/101.3-4.335

Hall, B. G., Betts, P. W., and Wootton, J. C. (1989). DNA sequence analysis of artificially evolved ebg enzyme and *ebg* repressor genes. *Genetics* 123, 635–648. doi: 10.1093/genetics/123.4.635

Hanson, A. D., Amthor, J. S., Sun, J., Niehaus, T. D., Gregory, J. F. III, Bruner, S. D., et al. (2018). Redesigning thiamin synthesis: prospects and potential payoffs. *Plant Sci.* 273, 92–99. doi: 10.1016/j.plantsci.2018.01.019

Hayashi, M., Kijima, Y., Tazuya-Murayama, K., and Yamada, K. (2015). The biosynthesis of the thiazole moiety of thiamin in the archaeon *Halobacterium salinarum*. *J. Nutr. Sci. Vitaminol.* 61, 270–274. doi: 10.3177/jnsv.61.27

Hayashi, M., Kobayashi, K., Esaki, H., Konno, H., Akaji, K., Tazuya, K., et al. (2014). Enzymatic andstructural characterization of an archaeal thiamine phosphate synthase. *Biochim. Biophys. Acta* 1844, 803–809. doi: 10.1016/j.bbapap.2014.02.017

Hsouna, A. B., Boye, A., Ackacha, B. B., Dhifi, W., Saad, R. B., Brini, F., et al. (2022). Thiamine demonstrates bio-preservative and anti-microbial effects in minced beef meat storage and lipopolysaccharide (LPS)-stimulated RAW 264.7 macrophages. *Animals* 12, 1646. doi: 10.3390/ani12131646

Hwang, S., Cordova, B., Abdo, M., Pfeiffer, F., and Maupin-Furlow, J. A. (2017). ThiN as a versatile domain of transcriptional repressors and catalytic enzymes of thiamine biosynthesis. *J. Bacteriol.* 199, e00810–e00816. doi: 10.1128/JB.00810-16

Hwang, S., Cordova, B., Chavarria, N., Elbanna, D., McHugh, S., Rojas, J., et al. (2014). Conserved active site cysteine residue of archaeal THI4 homolog is essential for thiamine biosynthesis in. *Haloferax volcanii*. *BMC Microbiol.* 14, 260. doi: 10.1186/s12866-014-0260-0

Hyatt, D., Chen, G. L., LoCascio, P. F., Land, M. L., Larimer, F. W., and Houser, L. J. (2010). Prodigal: prokaryotic gene recognition and translation initiation site identification. *BMC Bioinformatics* 11, 119. doi: 10.1186/1471-2105-11-119

Isenberg-Grzeda, E., Kutner, H. E., and Nicolson, S. E. (2012). Wernicke-korsakoff-syndrome: under-recognized and under-treated. *Psychosomatics* 53, 507–516. doi: 10.1016/j.psym.2012.04.008

Jenkins, A. H., Schyns, G., Potot, S., Sun, G., and Begley, T. P. (2007). A new thiamin salvage pathway. *Nat. Chem. Biol.* 3, 492–497. doi: 10.1038/nchembio.2007.13

Jurgenson, C. T., Begley, T. P., and Ealick, S. E. (2009). The structural and biochemical foundations of thiamin biosynthesis. *Annu. Rev. Biochem.* 78, 569–603. doi: 10.1146/annurev.biochem.78.072407.102340

Kanehisa, M., Sato, Y., and Morishima, K. (2016). BlastKOALA and GhostKOALA: KEGG tools for functional characterization of genome and metagenome sequences. *J. Mol. Biol.* 428, 726–731. doi: 10.1016/j.jmb.2015.11.006

Kappes, R., Kempf, B., and Bremer, E. (1999). Two evolutionarily closely related ABC transporters mediate the uptake of choline for synthesis of the osmoprotectant glycine betaine in *Bacillus subtilis*. *Mol. Microbiol.* 32, 203–216. doi: 10.1046/j.1365-2958.1999.01354.x

Kim, H. J., Lee, H., Lee, Y., Choi, I., Ko, Y., Lee, S., et al. (2020). The ThiL enzyme is a valid antibacterial target essential for both thiamine biosynthesis and salvage pathways in *Pseudomonas aeruginosa*. *J. Biol. Chem.* 295, 10081–10091. doi: 10.1074/jbc.RA120.013295

Kovács, N. (1956). Identification of *Pseudomonas pyocyanea* by the oxidase reaction. *Nature* 178, 703. doi: 10.1038/178703a0

Krzmarzick, M. J., Taylor, D. K., Fu, X., and McCutchan, A. L. (2018). Diversity and niche of archaea in bioremediation. *Archaea* 2018, 1–17. doi: 10.1155/2018/3194108

Larkin, M. A., Blackshields, G., Brown, N. P., Chenna, R., McGettigan, P. A., McWilliam, H., et al. (2007). Clustal W and clustal X version 2.0. *Bioinformatics* 23, 2947–2948. doi: 10.1093/bioinformatics/btm404

Lawhorn, B. G., Mehl, R. A., and Begley, T. P. (2004). Biosynthesis of the thiamin pyrimidine: the reconstitution of a remarkable rearrangement reaction. *Org. Biomol. Chem.* 2, 2538–2546. doi: 10.1039/B405429F

Lee, I., Kim, Y. O., Park, S. C., and Chun, J. (2016). OrthoANI: an improved algorithm and software for calculating average nucleotide identity. *Int. J. Syst. Evol. Microbiol.* 66, 1100–1103. doi: 10.1099/ijsem.0.000760

Ludwig, W., Strunk, O., Westram, R., Richter, L., Meier, H., Yadhukumar,, et al. (2004). ARB: a software environment for sequence data. *Nucleic Acids Res.* 32, 1363–1371. doi: 10.1093/nar/gkh293

Lv, P., Shang, Y., Zhang, Y., Wang, W., Liu, Y., Su, D., et al. (2022). Structural basis for the arsenite binding and translocation of Acr3 antiporter with NhaA folding pattern. *FASEB J.* 36, e22659. doi: 10.1096/fj.202201280R

Maguire, A., Simonelli, F., Pierce, E., Pugh, E., Mingozzi, F., Bennicelli, J., et al. (2008). Safety and efficacy of gene transfer for Leber's congenital amaurosis. *N. Engl. J. Med.* 358, 2240–2248. doi: 10.1056/NEJMoa0802315

Marmur, J. (1961). A procedure for the isolation of deoxyribonucleic acid from micro-organisms. *J. Mol. Biol.* 3, 208–218. doi: 10.1016/s0022-2836(61)80047-8

Maupin-Furlow, J. A. (2018). "Vitamin B1 (Thiamine) metabolism and regulation in archaea," in *B Group Vitamins-Current Uses and Perspectives*. Eds. J. G LeBlanc and G. S. de Giori (London: IntechOpen), 9–31. doi: 10.5772/intechopen.77170

Meier-Kolthoff, J. P., Sardà Carbasse, J., Peinado-Olarte, R. L., and Göker, M. (2022). TYGS and LPSN: a database tandem for fast and reliable genome-based classification and nomenclature of prokaryotes. *Nucleic Acids Res.* 50, 801–807. doi: 10.1093/nar/gkab902

Mojica, F. J. M., Díez-Villaseñor, C., García-Martínez, J., and Soria, E. (2005). Intervening sequences of regularly spaced prokaryotic repeats derive from foreign genetic elements. *J. Mol. Evol.* 60, 174–182. doi: 10.1007/s00239-004-0046-3

Montalvo-Rodríguez, R., Vreeland, R. H., Oren, A., Kessel, M., Betancourt, C., and López-Garriga, J. (1998). *Halogeometricum borinquense* gen. nov., sp. nov., a novel halophilic archaeon from Puerto Rico. *Int. J. Syst. Bacteriol.* 48, 1305–1312. doi: 10.1099/00207713-48-4-1305

Mrowicka, M., Mrowicki, J., Dragan, G., and Majsterek, I. (2023). The importance of thiamine (vitamin B1) in humans. *Biosci. Rep.* 43, BSR20230374. doi: 10.1042/BSR20230374

Müller, V., Spanheimer, R., and Santos, H. (2005). Stress response by solute accumulation in *Archaea*. *Curr. Opin. Microbiol.* 8, 729–736. doi: 10.1016/j.mib.2005.10.011

Multhaup, G., Strausak, D., Bissig, K.-D., and Solioz, M. (2001). Interaction of the CopZ copper chaperone with the CopA copper ATPase of *Enterococcus hirae* assessed by surface plasmon resonance. *Biochem. Biophys. Res. Commun.* 288, 172–177. doi: 10.1006/bbrc.2001.5746

Nieto, J. J., Ventosa, A., and Ruiz-Berraquero, F. (1987). Susceptibility of halobacteria to heavy metals. *Appl. Environ. Microbiol.* 53, 1199–1202. doi: 10.1128/aem.53.5.1199-1202.1987

Ordoñez, O. F., Rasuk, M. C., Soria, M. N., Contreras, M., and Farías, M. E. (2018). Haloarchaea from the Andean Puna: Biological role in the energy metabolism of arsenic. *Microb. Ecol.* 76, 695–705. doi: 10.1007/s00248-018-1159-3

Oren, A. (2011). "Diversity of halophiles," in *Extremophiles Handbook*. Ed. K. Horikoshi (Tokyo: Springer), 309–325.

Oren, A., Ventosa, A., and Grant, W. D. (1997). Proposed minimal standards for description of new taxa in the order *Halobacteriales*. *Int. J. Syst. Bacteriol.* 47, 233–238. doi: 10.1099/00207713-47-1-233

Ortigoza-Escobar, J. D., Molero-Luis, M., Arias, A., Oyarzabal, A., Darín, N., Serrano, M., et al. (2016). Free-thiamine is a potential biomarker of thiamine transporter-2 deficiency: a treatable cause of Leigh syndrome. *Brain* 139, 31–38. doi: 10.1093/brain/awv342

Overbeek, R., Olson, R., Pusch, G. D., Olsen, G. J., Davis, J. J., Disz, T., et al. (2014). The SEED and the Rapid Annotation of microbial genomes using Subsystems Technology (RAST). *Nucleic Acids Res.* 42, 206–214. doi: 10.1093/nar/gkt1226

Paltrinieri, T., Bondì, L., Đerek, V., Fraboni, B., Głowacki, E., and Cramer, T. (2021). Understanding photocapacitive and photofaradaic processes in organic semiconductor photoelectrodes for optobioelectronics. *Adv. Funct. Mater.* 31, 2010116. doi: 10.1002/adfm.202010116

Parks, D. H., Imelfort, M., Skennerton, C., Hugenholtz, P., and Tyson, G. W. (2015). CheckM: assessing the quality of microbial genomes recovered from isolates, single cells, and metagenomes. *Genome Res.* 25, 1043–1055. doi: 10.1101/gr.186072.114

Patel, R., Mevada, V., Prajapati, D., Dudhagara, P., Koringa, P., and Joshi, C. G. (2015). Metagenomic sequence of saline desert microbiota from wild ass sanctuary, little Rann of Kutch, Gujarat, India. *Genom. Data* 3, 137–139. doi: 10.1016/j.gdata.2015.01.003

Price, M. N., Dehal, P. S., and Arkin, A. P. (2010). FastTree 2–approximately maximum-likelihood trees for large alignments. *PloS One* 5, e9490. doi: 10.1371/journal.pone.0009490

Prjibelski, A., Antipov, D., Meleshko, D., Lapidus, A., and Korobeynikov, A. (2020). Using SPAdes *de novo* assembler. *Curr. Protoc. Bioinformatics* 70, e102. doi: 10.1002/cpbi.102

Qiu, X.-X., Zhao, M.-L., Han, D., Zhang, W.-J., Dyall-Smith, M. L., and Cui, H.-L. (2013). Taxonomic study of the genera *Halogeometricum* and *Halosarcina*: transfer of *Halosarcina limi* and *Halosarcina pallida* to the genus *Halogeometricum* as *Halogeometricum limi* comb. nov. and *Halogeometricum pallidum* comb. nov., respectively. *Int. J. Syst. Evol. Microbiol.* 63, 3915–3919. doi: 10.1099/ijs.0.055038-0

Rensing, C., Fan, B., Sharma, R., Mitra, B., and Rosen, B. P. (2000). CopA: an *Escherichia coli* cu(I)-translocating P-type ATPase. *Res. Microbiol.* 151, 597–603. doi: 10.1016/S0923-2508(00)01129-0

Rensing, C., Mitra, B., and Rosen, B. P. (1997). The *zntA* gene of *Escherichia coli* encodes a Zn(II)- translocating P-type ATPase. *Proc. Natl. Acad. Sci. U.S.A.* 94, 14326–14331. doi: 10.1073/pnas.94.26.14326

Ribeiro, T., Fonseca, F. L., de Carvalho, M. D. C., Godinho, R. M. C., de Almeida, F. P., Saint'Pierre, T., et al. (2017). Metal-based superoxide dismutase and catalase mimics reduce oxidative stress biomarkers and extend life span of *Saccharomyces cerevisiae*. *Biochem. J.* 474, 301–315. doi: 10.1042/BCJ20160480

Rice, P., Longden, L., and Bleasby, A. (2000). EMBOSS: the European Molecular Biology Open Software Suite. *Trends Genet.* 16, 276–277. doi: 10.1016/S0168-9525(00)02024-2

Richards, L. (1954). "Diagnosis and improvement of saline and alkali soils," in *Agriculture Handbook no. 60* (Washington, DC: US Government Printing Office).

Richter, M., and Rossello-Mora, R. (2009). Shifting the genomic gold standard for the prokaryotic species definition. *Proc. Natl. Acad. Sci. U.S.A.* 106, 19126–19131. doi: 10.1073/pnas.0906412106

Riesco, R., and Trujillo, M. E. (2024). Update on the proposed minimal standards for the use of genome data for the taxonomy of prokaryotes. *Int. J. Syst. Evol. Microbiol.* 74, 6300. doi: 10.1099/ijsem.0.006300

Rodionov, D. A., Leyn, S. A., Li, X., and Rodionova, I. A. (2017). A novel transcriptional regulator related to thiamine phosphate synthase controls thiamine metabolism genes in archaea. *J. Bacteriol.* 199, e00743–e00716. doi: 10.1128/JB.00743-16

Rodionov, D. A., Vitreschak, A. G., Mironov, A. A., and Gelfand, M. S. (2002). Comparative genomics of thiamin biosynthesis in procaryotes. New genes and regulatory mechanisms. *J. Biol. Chem.* 277, 48949–48959. doi: 10.1074/jbc.M208965200

Rodríguez-R, L. M., and Konstantinidis, K. T. (2016). The Enveomics collection: a toolbox for specialized analyses of microbial genomes and metagenomes. *PeerJ Preprints* 4, e1900v1. doi: 10.7287/peerj.preprints.1900v1

Rodríguez-Valera, F. (1988). "Characteristics and microbial ecology of hypersaline environments," in *Halophilic bacteria*. Ed. F. Rodríguez-Valera (Boca Raton: CRC Press), 3–30.

Rouvrais, C., Baspeyras, M., Mengeaud, V., and Rossi, A. (2018). Antiaging efficacy of a retinaldehyde-based cream compared with glycolic acid peel sessions: A randomized controlled study. *J. Cosmet Dermatol.* 17, 1136–1143. doi: 10.1111/jocd.12511

Saitou, N., and Nei, M. (1987). The neighbor-joining method: a new method for reconstructing phylogenetic trees. *Mol. Biol. Evol.* 4, 406–425. doi: 10.1093/oxfordjournals.molbev.a040454

Sathe, R. R. M., Paerl, R. W., and Hazra, A. B. (2022). Exchange of vitamin B_1 and its biosynthesis intermediates shapes the composition of synthetic microbial cocultures and reveals complexities of nutrient sharing. *J. Bacteriol.* 204, e005032. doi: 10.1128/jb.00503-21

Savage, K. N., Krumholz, L. R., Oren, A., and Elshahed, M. S. (2008). *Halosarcina pallida* gen. nov., sp. nov., a halophilic archaeon from a low-salt, sulfide-rich spring. *Int. J. Syst. Evol. Microbiol.* 58, 856–860. doi: 10.1099/ijs.0.65398-0

Seemann, T. (2014). Prokka: rapid prokaryotic genome annotation. *Bioinformatics* 30, 2068–2069. doi: 10.1093/bioinformatics/btu153

Serrano, S., Mendo, S., and Caetano, T. (2022). Haloarchaea have a high genomic diversity for the biosynthesis of carotenoids of biotechnological interest. *Res. Microbiol.* 173, 103919. doi: 10.1016/j.resmic.2021.103919

Sheikh, S., O'Handley, S. F., Dunn, C. A., and Bessman, M. J. (1998). Identification and characterization of the Nudix hydrolase from the archaeon, *Methanococcus jannaschii*, as a highly specific ADP-ribose pyrophosphatase. *J. Biol. Chem.* 273, 20924–20928. doi: 10.1074/jbc.273.33.20924

Srivastava, P., and Kowshik, M. (2013). Mechanisms of metal resistance and homeostasis in haloarchaea. *Archaea* 2013, 732864. doi: 10.1155/2013/732864

Straková, D., Sánchez-Porro, C., de la Haba, R. R., and Ventosa, A. (2024). Decoding the genomic profile of the *Halomicroarcula* genus: comparative analysis and characterization of two novel species. *Microorganisms* 12, 334. doi: 10.3390/microorganisms12020334

Subov, N. N. (1931). "Oceanographical tables. Comissariat of agriculture of USSR," in *Hydro-meteorogical committee of USSR* (Moscow: Oceanographical Institute of USSR).

Sun, J., Sigler, C. L., Beaudoin, G. A. W., Joshi, J., Patterson, J. A., Cho, K. H., et al. (2019). Parts-prospecting for a high-efficiency thiamin thiazole biosynthesis pathway. *Plant Physiol.* 179, 958–968. doi: 10.1104/pp.18.01085

Taskiran, A. S., and Ergul, M. (2021). The modulator action of thiamine against pentylenetetrazole-induced seizures, apoptosis, nitric oxide, and oxidative stress in rats and SH-SY5Y neuronal cell line. *Chem. Biol. Interact.* 340, 109447. doi: 10.1016/J.CBI.2021.109447

Tavoosi, N., Akhavan Sepahi, A., Amoozegar, M. A., and Kiarostami, V. (2023). Toxic heavy metal/oxyanion tolerance in haloarchaea from some saline and hypersaline ecosystems. *J. Basic. Microbiol.* 63, 558–569. doi: 10.1002/jobm.202200465

Tchounwou, P. B., Yedjou, C. G., Patlolla, A. K., and Sutton, D. J. (2012). Heavy metal toxicity and the environment. *Exp. Suppl.* 101, 133–164. doi: 10.1073/pnas.0506758102

Tettelin, H., Masignani, V., Cieslewicz, M. J., Donati, C., Medini, D., Ward, N. L., et al. (2005). Genome analysis of multiple pathogenic isolates of *Streptococcus agalactiae*: Implications for the microbial "pan-genome". *Proc. Natl. Acad. Sci. U.S.A.* 102, 13950–13955. doi: 10.1073/pnas.0506758102

Torreblanca, M., Rodriguez-Valera, F., Juez, G., Ventosa, A., Kamekura, M., and Kates, M. (1986). Classification of non-alkaliphilic halobacteria based on numerical taxonomy and polar lipid composition, and description of *Haloarcula* gen. nov. and *Haloferax* gen. nov. *Syst. Appl. Microbiol.* 8, 89–99. doi: 10.1016/S0723-2020(86)80155-2

Trojańska, M., Rogala, M., Kowalczyk, A., Chyc, M., Latowski, D., and Bojko, M. (2022). Is the merA gene sufficient as a molecular marker of mercury bacterial resistance. *Acta Biochim. Pol.* 69, 507–512. doi: 10.18388/abp.2020_6399

Ventosa, A. (2006). "Unusual micro-organisms from unusual habitats: hypersaline environments," in *Prokaryotic diversity: mechanisms and significance*. Eds. N. A. Logan, H. M. Lappin-Scrott and P. C. F. Oyston (Cambridge: Cambridge University Press), 223–254.

Ventosa, A., Mellado, E., Sánchez-Porro, C., and Márquez, M. C. (2008). "Halophilic and halotolerant micro-organisms from soils," in *Microbiology of extreme soils*. Eds. P. Dion and C. S. Nautiyal (Berlin: Springer), 87–115. doi: 10.1007/978-3-540-74231-9_5

Vera-Bernal, M., and Martínez-Espinosa, R. M. (2021). Insights on cadmium removal by bioremediation: the case of haloarchaea. *Microbiol. Res.* 12, 354–375. doi: 10.3390/microbiolres12020024

Vera-Gargallo, B., Chowdhury, T. R., Brown, J., Fansler, S. J., Durán-Viseras, A., Sánchez-Porro, C., et al. (2019). Spatial distribution of prokaryotic communities in hypersaline soils. *Sci. Rep.* 9, 1769. doi: 10.1038/s41598-018-38339-z

Vera-Gargallo, B., Navarro-Sampedro, L., Carballo, M., and Ventosa, A. (2018). Metagenome sequencing of prokaryotic microbiota from two hypersaline soils of the Odiel Salt Marshes in Huelva, Southwestern Spain. *Genome Announc.* 6, e00140–e00118. doi: 10.1128/genomeA.00140-18

Vera-Gargallo, B., and Ventosa, A. (2018). Metagenomic insights into the phylogenetic and metabolic diversity of the prokaryotic community dwelling in hypersaline soils from the Odiel Saltmarshes (SW Spain). *Genes* 9, 152. doi: 10.3390/genes9030152

Voica, D. M., Bartha, L., Banciu, H. L., and Oren, A. (2016). Heavy metal resistance in halophilic Bacteria and Archaea. *FEMS Microbiol. Lett.* 363, fnw146. doi: 10.1093/femsle/fnw146

Wilson, R. B. (2020). Pathophysiology, prevention, and treatment of beriberi after gastric surgery. *Nutr. Rev.* 78, 1015–1029. doi: 10.1093/nutrit/nuaa004

Yan, Y., and Moult, J. (2006). Detection of operons. *Proteins* 64, 615–628. doi: 10.1002/prot.21021

Yoon, S.-H., Ha, S.-M., Kwon, S., Lim, J., Kim, Y., Seo, H., et al. (2017). Introducing EzBioCloud: a taxonomically united database of 16S rRNA gene sequences and whole-genome assemblies. *Int. J. Syst. Evol. Microbiol.* 67, 1613–1617. doi: 10.1099/ijsem.0.001755

Youssef, N. H., Savage-Ashlock, K. N., McCully, A. L., Luedtke, B., Shaw, E. I., Hoff, W. D., et al. (2014). Trehalose/2-sulfotrehalose biosynthesis and glycine-betaine uptake are widely spread mechanisms for osmoadaptation in the *Halobacteriales*. *ISME J.* 8, 636–649. doi: 10.1038/ismej.2013.165

Zhang, X., Eser, B. E., Chanani, P. K., Begley, T. P., and Ealick, S. E. (2016). Structural basis for iron-mediated sulfur transfer in archael and yeast thiazole synthases. *Biochemistry* 55, 1826–1838. doi: 10.1021/acs.biochem.6b00030

Zhao, Y., Jia, X., Yang, J., Ling, Y., Zhang, Z., Yu, J., et al. (2014). PanGP: A tool for quickly analyzing bacterial pan-genome profile. *Bioinformatics* 30, 1297–1299. doi: 10.1093/bioinformatics/btu017